Poznan University of Technology
Faculty of Machines and Transportation

MASTER'S THESIS

SIMULATION AND NUMERICAL ANALYSIS OF FLUID FLOW IN SYSTEMS OF RENEWABLE WIND ENERGY

Poznań 2016

Promoter: **Tomasz STRĘK, PhD. Eng.**

Poznan University of Technology
INSTITUTE OF APPLIED MECHANICS
FACULTY OF MECHANICAL ENGINEERING & MANAGEMENT

TABLE OF CONTENT

Table of content **7**
ABSTRACT **9**
1. Renewable Energy **11**
1.1.Renewable Wind Energy 11
1.1.1. Energy generation by Wind Turbine 12
2. INVELOX **15**
3. Navier-Stock Equation - Equation of Motion of a Viscous Fluid **17**
4. Navier-Stock Equation – Non-dimensional Form **23**
5. Similarity of Flows **27**
6. Mathematical Description of Model 1 ..... **29**
7. SImulation Methodology of Model 1 ..... **31**
8. Results of Simulation of Model 1 ..... **37**
8.1.Time independent study 37
8.1.1. Parameters of inlets velocities: U_wind=0.9, U_wind2=0.1 37
8.1.2. Parameters of inlets velocities: U_wind=0.1, U_wind2=0.9. 41
8.1.3. Parameters of inlets velocities: U_wind=0.6, U_wind2=0.4 44
8.2.Time dependent study 46
8.2.1. Results of simulation 47
9. Mathematical Description of Model 2 ..... **51**
10. Results of Simulation of Model 2 ..... **55**
10.1. Time independent study. 55
10.2. Time dependent study 56
11. Comparision of Results **59**
12. Conslusions **61**
BIBLIOGRAPHY **63**
STRESZCZENIE **65**

ABSTRACT

In the first section of thesis, the forecast for the development of Renewable Energy, particularly Renewable Wind Energy, on the World was discussed. Then the mode of operation of the wind turbine was presented. In second chapter Renewable Wind Energy system – INVELOX was described. In next chapters the Navier-Stock equation and way of programming in COMSOL Multiphysics was presented. Later the models 2D and 3D and the simulation were presented. At the end of the thesis the results of simulations and conclusions are described.

1. RENEWABLE ENERGY

In times of increasing public awareness on the impact of humanity on the degradation of the environment, the greater importance is given to protect it. Mainly attempts were made to reduce emissions and the consumption of non-renewable energy sources. The sector of green energy production is classed as a low-carbon economy, which is one of the most important elements of a green economy. Some sectors of renewable energy, such as wind power, solar energy or agricultural biogas plants, note the increase in the market at a rate of 30-50% per annum. In the conditions of the European Union climate package "3x20%" and Directive 2009/28/EC about the promotion of the use of energy from renewable sources, the high growth rate should be maintained throughout the decade. Poland in 2020 will be able to achieve the minimum 15% share of green energy in the balance of consumption [Figure 1.1].

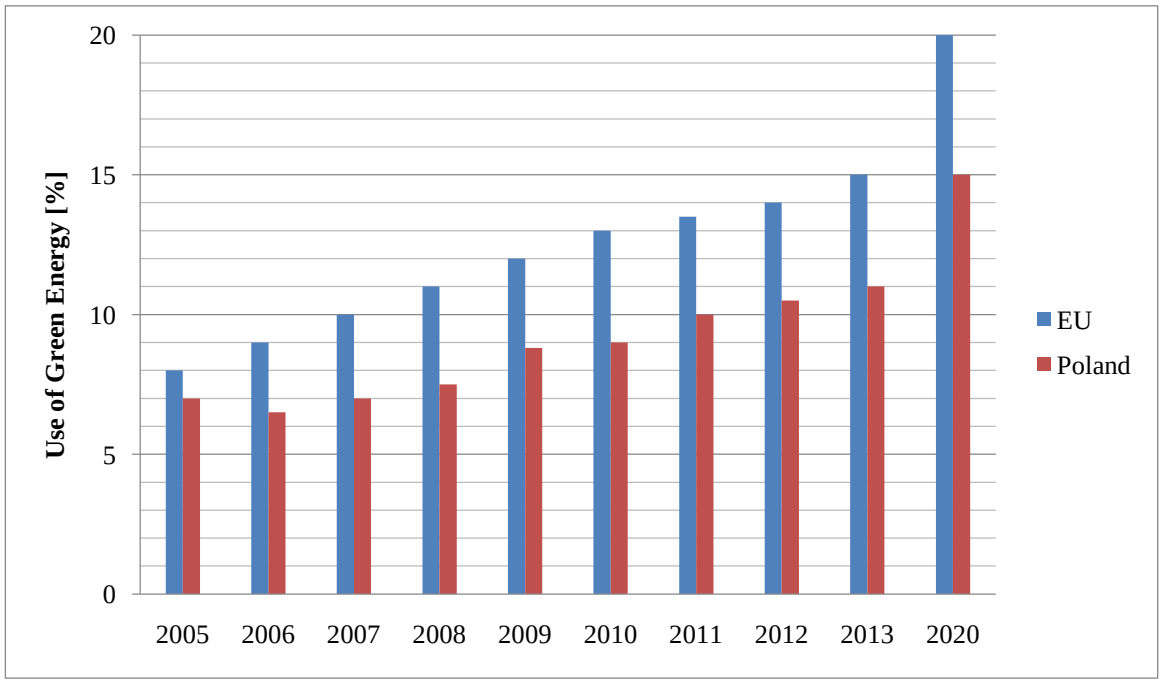

Figure 1.1 - The share of Renewable Energy in gross final consumptions – Europe 2020 indicators

1.1. Renewable Wind Energy

Wind power is one of the cheapest technological options to reduce emissions CO_2. According to the developed plan, the reduction of CO_2 emissions through wind power will reached 33 million tons in 2020., with further growth potential to 65 million tons in 2030.

From among sources of renewable energies on the world the renewable wind energy develops the best. In 2013 in EU the Wind Energy accounted more than 10.5% from all sources of renewable energies.

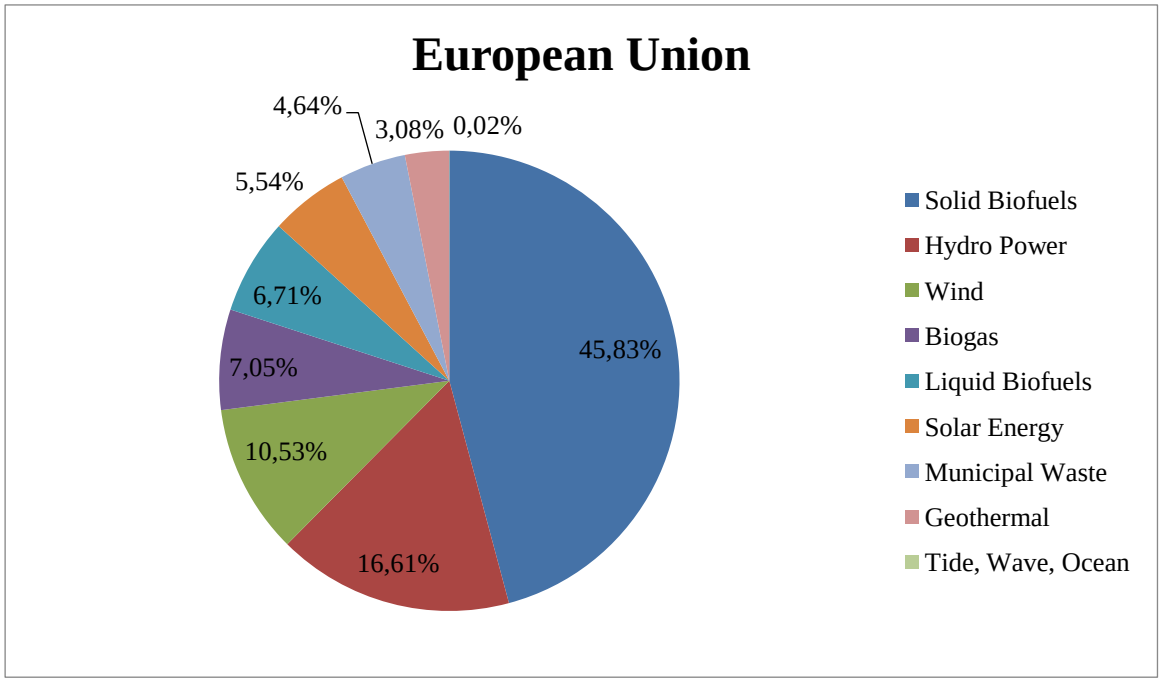

Figure 1.2 - The share of renewable commodities in the total obtaining primary energy from renewable sources in 2013 in European Union

Large wind turbines (in practice over 100 kW), except that it can be supplied to house, are primarily used to generate electricity, which is sold to the power grid. Modern large wind power plants is deposited on the towers with high of 70-120 meters.

1.1.1. Energy generation by Wind Turbine

Wind is formed by temperature difference of air masses which are caused by uneven heating of Earth's surface. The wind turbine is able to generate the power by converting wind through the torque acting on the rotor blades. The rotor is mounted on the shaft drives the electric generator. The rotors rotates at a speed of 15-20 rev/min, whereas a typical asynchronous generator produces electricity at a speed of 1500 rev/min. It is necessary to use a gear box, which is made to increase the rotational speed. The most effective and most commonly used are three-bladed turbines. In the hub of the rotor the servomechanism is located to allow the setting of the inclination of the rotors blade. The top of the tower is installed on the engine which can be rotated by a gear. Air flow incoming to the rotor of the

blades causes rotational movement of the rotor. The energy of the rotating rotor can be used directly to power mechanical devices or by coupling a generator to produce electricity.

Wind turbines use wind power in terms of the speed of 4 to 25 m/s. At wind speeds above 25 m/s for safety reasons the plant is stopped.

The parameters of the turbine (e.g. the speed of rotation, the incidence angle of blades) are controlled by 24-hours by the monitoring systems. This is necessary in order to protect the turbine from damage and to ensure optimum operating conditions. In case of extreme weather conditions turbine alone is set, with the wind, adjusts the angle of the blades and block the drive mechanisms.

2. INVELOX

Efficiency of conversion of wind to energy by wind turbine is determined by the parameters like the free stream wind speed and blade shape orientation and radius of blades. According to these design parameters, the height of tower and the diameter of blades have grown to sizes that are considered inflated in conventional systems and which are very challenging according to logistic, manufacturing or installation.

INVELOX is a system which increase a wind speed. It consist shaped funnel with omnidirectional inlet (1) where the wind intakes and go through all system. The crucial element is Venturi (4) where wind speed is concentrated and accelerated.

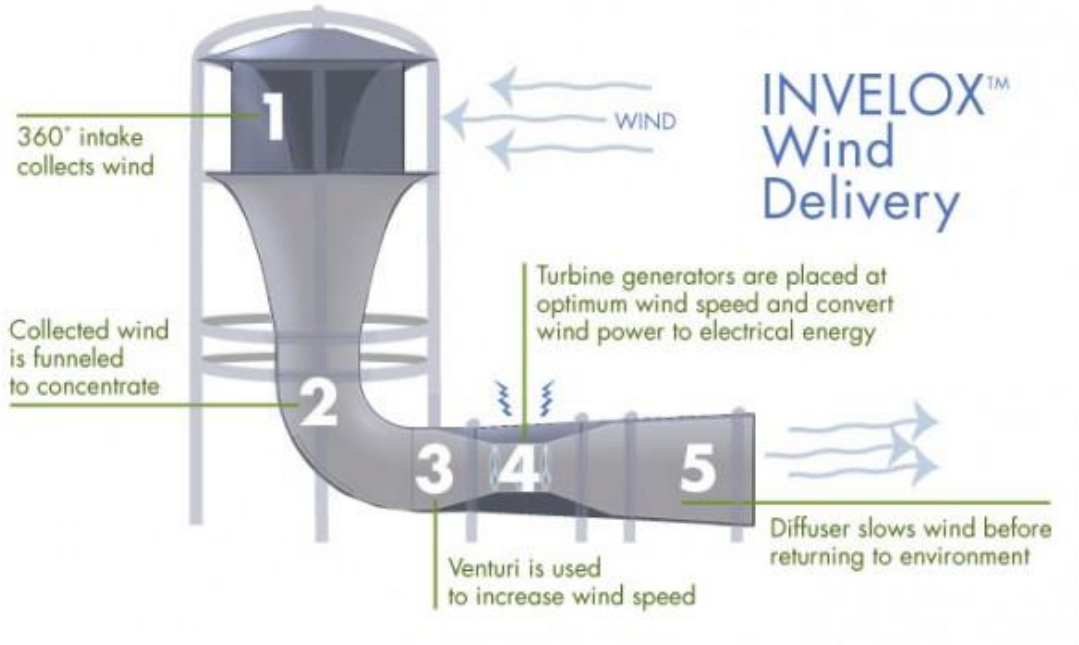

Figure 2.1 - Construction of INVELOX system from http://pacificwind.co.nz/

According to the Sheer Wind company, the creator of the INVELOX, this system is six times more efficient than the turbine. The company conducted internal tests and compared INVELOX and turbine. The results shows the improving of energy production ranges from 81-660%.

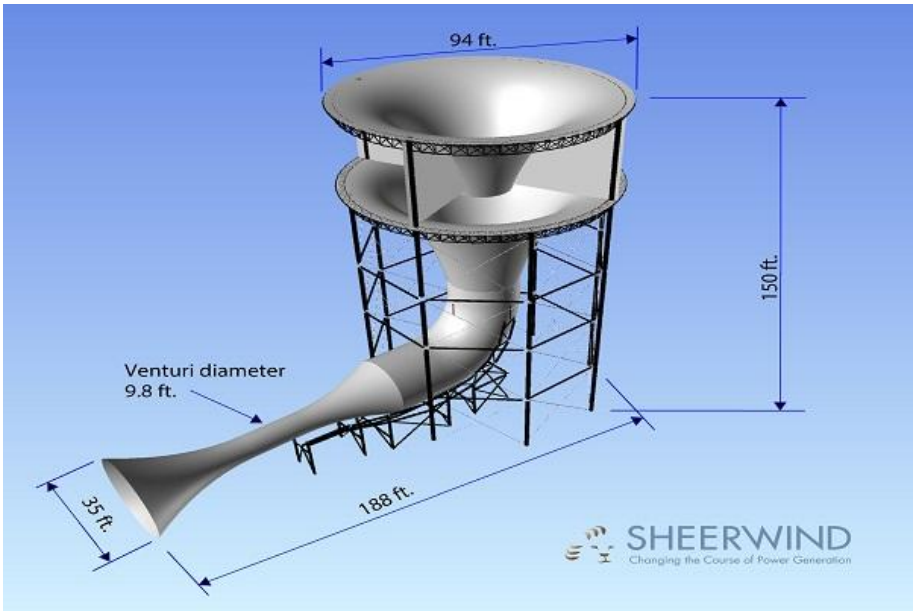

Figure 2.2 - Scheme of INVELOX system from http://pacificwind.co.nz/

The pivotal cons for environment is an elimination of need of high tower turbines with rotating blades which emit nagging vibration and noise or which are the reason of flickering lights effect.

Rotating turbine blades are at the ceiling height of the flight of birds. this creates a risk of collision. In INVELOX system the blades are hidden in the cover.

3. NAVIER-STOCK EQUATION - EQUATION OF MOTION OF A VISCOUS FLUID [3]

Euler's equation is an balance of equilibrium of forces acting on the fluid, and it is called the dynamic condition of a flow capabilities. Euler's equation for a perfect fluid expresses the condition of equilibrium of forces of inertia, mass and pressure:

$$\frac{D\vec{U}}{Dt} = \vec{F} - \frac{1}{\rho} grad\ p. \tag{3.1}$$

If in a motion of fluid we take into account the fluid viscosity, in the equation instead of the pressure force will be the surface force $\vec{P}$. The surface force will contain a normal component P_n and a tangential component P_s.

$$\vec{P} = P_n\vec{n} + P_s\vec{s} \tag{3.2}$$

After consideration of that relationship, we can overwrite the equation (3.1) in the form:

$$\rho\frac{D\vec{U}}{dt} = \rho\vec{F} + \vec{P} \tag{3.3}$$

Normal component and the tangential component of the surface force are expressed by tension, which means the forces relative to the area unit in accordance with the following convention:

$$P_n = \sigma_n \cdot S$$
$$P_s = \tau_{ns} \cdot S$$

where: n index denotes the normal direction to surface and s index the direction along which acts the shear stress.

If we consider the description of the fluid element equilibrium in Cartesian coordinates, then the force the surface occurs in equation (3.3) we will be able to save as follows:

$$\vec{P} = P_x\vec{\imath} + P_y\vec{\jmath} + P_z\vec{k} \tag{3.4}$$

The relevant fluid element is subjected to compression by the surrounding elements, and therefore the normal stress σ will represent the reaction of the fluid element to the

surroundings and they will be directed to the outside. On the surface dxdz act the tension, which along the y-axis will exhibit an increase (gradient) respectively equal to:

$$\frac{\partial \tau_{yz}}{\partial y} : \frac{\partial \tau_{yx}}{\partial y}$$

The surface force related to the unit volume, which, after taking into account the relation (3.4) can be written:

$$P_x = \frac{\partial \sigma_x}{\partial x} + \frac{\partial \sigma_{yx}}{\partial y} + \frac{\partial \sigma_{zx}}{\partial z}$$
$$P_y = \frac{\partial \sigma_y}{\partial y} + \frac{\partial \sigma_{xy}}{\partial x} + \frac{\partial \sigma_{yz}}{\partial z}$$
$$P_z = \frac{\partial \sigma_z}{\partial z} + \frac{z}{\partial y} + \frac{\partial \sigma_{xz}}{\partial x}$$

After consideration of this dependency in equations (3.3) and (3.4) the equation of motion of viscous fluid can be written as:

$$\frac{DU_x}{Dt} = X + \frac{1}{\rho}\left(\frac{\partial \sigma_x}{\partial x} + \frac{\partial \tau_{yx}}{\partial y} + \frac{\partial \tau_{zx}}{\partial z}\right)$$
$$\frac{DU_y}{Dt} = Y + \frac{1}{\rho}\left(\frac{\partial \sigma_y}{\partial y} + \frac{\partial \tau_{xy}}{\partial x} + \frac{\partial \tau_{yx}}{\partial z}\right) \qquad (3.5)$$
$$\frac{DU_z}{Dt} = Z + \frac{1}{\rho}\left(\frac{\partial \sigma_z}{\partial z} + \frac{\partial \tau_{yz}}{\partial y} + \frac{\partial \tau_{xz}}{\partial x}\right)$$

Normal stress σ cause strain ε volumetric and shear stress τ cause deformation of amorphous λ.

- Deformation volume:

$$\varepsilon_x = \frac{\partial U_x}{\partial x}$$
$$\varepsilon_y = \frac{\partial U_y}{\partial y}$$
$$\varepsilon_z = \frac{\partial U_z}{\partial z}$$

- Non-dilatational strain:

$$\lambda_{xy} = \lambda_{yx} = \left(\frac{\partial U_x}{\partial y} + \frac{\partial U_y}{\partial x}\right)$$
$$\lambda_{yz} = \lambda_{zy} = \left(\frac{\partial U_y}{\partial z} + \frac{\partial U_z}{\partial y}\right)$$

$$\lambda_{xz} = \lambda_{zx} = \left(\frac{\partial U_x}{\partial z} + \frac{\partial U_z}{\partial x}\right)$$

From Newton's equation

$$\tau = \mu \frac{dU}{dy} \tag{3.6}$$

result that the coefficient of proportionality between the stress and tangential velocity gradient is the viscosity coefficient μ. It allows to save the shear stress occurring in the equation (3.5) in the following form:

$$\begin{aligned} \tau_{xy} &= \tau_{yx} = \mu\left(\frac{\partial U_x}{\partial y} + \frac{\partial U_y}{\partial x}\right) \\ \tau_{yz} &= \tau_{zy} = \mu\left(\frac{\partial U_y}{\partial z} + \frac{\partial U_z}{\partial y}\right) \\ \tau_{xz} &= \tau_{zx} = \mu\left(\frac{\partial U_{zx}}{\partial x} + \frac{\partial U_x}{\partial z}\right) \end{aligned} \tag{3.7}$$

If we assume that the deformation of the right angle formed by the walls of the fluid element is the sum of deformation dα + dβ and therefore can introduce the concept of average speed angular deformation:

$$\begin{aligned} \left(\lambda_{xy}\right)_{av} &= \left(\lambda_{yx}\right)_{av} = \frac{1}{2}\left(\frac{\partial U_y}{\partial x} + \frac{\partial U_x}{\partial y}\right) \\ \left(\lambda_{yz}\right)_{av} &= \left(\lambda_{zy}\right)_{av} = \frac{1}{2}\left(\frac{\partial U_z}{\partial y} + \frac{\partial U_y}{\partial z}\right) \\ (\lambda_{xz})_{av} &= (\lambda_{zx})_{av} = \frac{1}{2}\left(\frac{\partial U_x}{\partial z} + \frac{\partial U_z}{\partial x}\right) \end{aligned} \tag{3.8}$$

Only in this case, the dependency (3.7) will be accordance with Newton law, so the factor of proportionality of stress to the average strain rate will be equal:

$$\tau = 2\mu\, \lambda_{av} \tag{3.9}$$

In the case of normal stresses σ present in the formula (3.5), we assume that in case of non-viscous fluid they would be equal to the pressure:

$$\sigma_x = \sigma_y = \sigma_z = -p$$

In the viscous fluid the normal stresses would be the sum of pressure and additional stresses caused by viscosity:

$$\sigma_x = -p + \acute{\sigma}_x$$
$$\sigma_y = -p + \acute{\sigma}_y \quad (3.10)$$
$$\sigma_z = -p + \acute{\sigma}_z$$

At every point of viscous fluid must be defined so the pressure stress must comply with the definitional relationship:

$$\frac{\sigma_z + \sigma_y + \sigma_y}{3} = -p \quad (3.10)$$

We assume that additional stresses give value equal zero. They come from the viscosity, so it must be assumed that the coefficient of proportionality of those stress of deformation will be the same as in the case of shear stresses:

$$\acute{\sigma}_x = 2\mu\varepsilon_x$$
$$\acute{\sigma}_y = 2\mu\varepsilon_y \quad (3.11)$$
$$\acute{\sigma}_z = 2\mu\varepsilon_z$$

This dependence is real for incompressible fluid, because we assumed that additional stresses give value equal zero:

$$\acute{\sigma}_x + \acute{\sigma}_y + \acute{\sigma}_z = 2\mu(\varepsilon_x + \varepsilon_y + \varepsilon_z) = 2\mu\left(\frac{\partial U}{\partial x} + \frac{\partial U}{\partial y} + \frac{\partial U}{\partial z}\right) = 2\mu\ div\ \vec{U}$$

To the divergence of the velocity vector equals zero

$$div\ \vec{U} = 0$$

means that the fluid must be incompressible.

If the relationship (3.10) would be important for the general case, that means for compressible and incompressible fluids, the relationship (3.10) should be written in the form:

$$\sigma_x = -p + 2\mu\varepsilon_x + \lambda\ div\ \vec{U}$$
$$\sigma_y = -p + 2\mu\varepsilon_y + \lambda\ div\ \vec{U} \quad (3.12)$$
$$\sigma_z = -p + 2\mu\varepsilon_z + \lambda\ div\ \vec{U}$$

where

$$\lambda\ div\ \vec{U}$$

means additional stressed proportional to unit changes of volume $\vec{U}$ compressible fluid. Ratio of proportionality λ is unknown and it should be determine from condition (3.10) which must be fulfilled also to incompressible liquid. Substitution of (3.12) to (3.10) let us to overwrite:

$$\frac{1}{3}\left[-3p + 2\mu\left(\frac{\partial U_x}{\partial x} + \frac{\partial U_y}{\partial y} + \frac{\partial U_z}{\partial z}\right) + 3\lambda\, div\, \vec{U}\right] = -p$$

and after transformation:

$$2\mu\, div\, \vec{U} + 3\lambda\, div\vec{U} = 0$$

Taking into account that for incompressible liquid

$$div\, \vec{U} \neq 0$$

It is possible to divide both sides by this value:

$$2\mu+3\lambda=0$$

Finally we get the value of proportionality factor:

$$\lambda = -\frac{2}{3}\mu$$

What after substitution to equation (3.12) let to overwrite the equation which determines normal tension in viscous fluid:

$$\begin{aligned} \sigma_x &= -p + 2\mu\varepsilon_x - \frac{2}{3}\,\mu\, div\, \overrightarrow{U} \\ \sigma_y &= -p + 2\mu\varepsilon_y - \frac{2}{3}\,\mu\, div\, \overrightarrow{U} \\ \sigma_z &= -p + 2\mu\varepsilon_z - \frac{2}{3}\,\mu\, div\, \overrightarrow{U} \end{aligned} \qquad (3.13)$$

Substituting equations (3.13) and (3.7) to relation (3.5) we get the equation of viscous fluid motion, which as traces on three axes can be written like follow

$$\begin{aligned} \frac{DU_y}{Dt} &= Y - \frac{1}{\rho}\frac{\partial p}{\partial y} + v\nabla^2 \mathrm{U_y} + \frac{2}{3}v\frac{\partial}{\partial \mathrm{y}}\left(\mathrm{div}\vec{\mathrm{U}}\right), \\ \frac{DU_z}{Dt} &= Z - \frac{1}{\rho}\frac{\partial p}{\partial z} + v\nabla^2 \mathrm{U_z} + \frac{2}{3}v\frac{\partial}{\partial \mathrm{z}}\left(\mathrm{div}\vec{\mathrm{U}}\right), \end{aligned} \qquad (3.14)$$

or in the vector form:

$$\frac{D\vec{U}}{Dt} = \vec{F} - \frac{1}{\rho}grad\ p + v\nabla^2\vec{\mathrm{U}} + \frac{2}{3}v\,\mathrm{grad}\left(\mathrm{div}\vec{\mathrm{U}}\right). \qquad (3.15)$$

Formulas (3.14) and (3.15) are called *Navier-Stokes equations*. Equation (3.15) can be simplified if the flow of liquid, for which you can ignore the influence of compressibility will be considered:

$$\frac{D\vec{U}}{Dt} = \vec{F} - grad\ p + v\nabla^2\overrightarrow{\mathrm{U}}. \tag{3.16}$$

In case of fluid flow with moderate velocity (Ma < 0.3) in addition to the forces of compressibility the mass forces can be also skipped, because the force mass is balanced by hydrostatic pressure. Therefore, if the pressure p the hydrodynamic pressure equals the difference between the total pressure and hydrostatic pressure, the *Navier-Stokes equation* can be saved as follows:

$$\frac{D\vec{U}}{Dt} = -\frac{1}{\rho}grad\ p + v\nabla^2\vec{\mathrm{U}}. \tag{3.17}$$

Navier-Stokes equation contains the same number of unknowns as Euler's equation and It must also be supplemented by the continuity equation and the equation of state. Like the Euler equation and also the Navier-Stokes equations must be supplemented with initial and boundary conditions, and the complexity of the boundary conditions in this case is much higher.

4. NAVIER-STOCK EQUATION – NON-DIMENSIONAL FORM [3]

Taking into account how complicated Computational Fluid Mechanics can be, sometimes more beneficial is to write governing equations in non-dimensional form. To do this we need to select a characteristic quantities that describe the flow problem, such as a characteristic length, characteristic velocity, characteristic pressure and characteristic temperature . Using these characteristic quantities the following non-dimensional parameters can be defined.

For specific problem a characteristic size D and the characteristic speed U_wind has been determined. The value D it is a diameter of venturi section. Rest of the INVELOX system dimensions was determined by scaling of model in reference to D value which equals 1 (scaled model – Figure 6.1).

Dimensionless variables:

Length scales:

$$x^* = \frac{x}{D}, y^* = \frac{y}{D}, z^* = \frac{z}{D},$$

where D is a characteristic dimension.

$$\nabla^* = D\nabla$$

Laplacian:

$$\nabla^{*2} = D^2\nabla^2,$$

Time scales:

$$t^* = \frac{t}{t_{rf}},$$

$$t_{rf} = \frac{D}{U},$$

Where U is a characteristic velocity,

Velocity scales:

$$\vec{v}^* = \frac{\vec{v}}{U},$$

Pressure scales:

$$p^* = \frac{p}{\eta \cdot \frac{U}{D}}$$

Dimensionless $Re = \frac{\rho v_0 L_o}{\mu}$ $\frac{inertia}{viscosity}$

numbers:Reynolds number

Froude number	$Re = \frac{v_0}{\sqrt{L_0 g}}$	$\frac{inertia}{gravity}$
Strouhal number	$St = \frac{L_0}{v_0 t_0}$	Describes oscillating flow mechanisms.

$$\frac{\rho U}{t_{rf}} \cdot \frac{\partial \vec{v}^*}{\partial t^*} + \frac{\rho U}{D} \cdot \vec{v}^* \cdot \nabla^* \vec{U}^* = \frac{-\eta U}{D^2} \nabla^* \rho^* + \eta \frac{U}{D^2} \nabla^{*2}$$

$$\frac{\rho UD}{\eta} \cdot \frac{D}{U \cdot t_{rf}} \cdot \frac{\partial \vec{v}^*}{\partial t^*} + \frac{\rho UD}{\eta} \vec{u}^* \cdot \nabla^* \vec{v}^* = -\nabla^* \rho^* + \nabla^{*2} \vec{u}^2$$

$$\frac{\rho UD}{\eta} = Re$$

$$\frac{D}{U \cdot t_{rf}} = \frac{1}{St}$$

$$\frac{t_{rf}}{D/U} = St$$

$$\frac{Re}{St} \cdot \frac{\partial \vec{v}^*}{\partial t^*} + Re\, \vec{u}^* = -\nabla^* \rho^* + \nabla^{*2}\, \vec{u}^*$$

$$\nabla^* \rho^* = \nabla^{*2}\, \vec{u}^*$$

$$\nabla \rho = \eta \nabla^2 \vec{u}$$

Stationary non-dimensional Navier-Stokes equation can be written as:

$$\begin{cases} (u \cdot \nabla)u = \nabla \cdot \left[-pI + \frac{1}{Re} (\nabla u + (\nabla u)^T - \frac{2}{3} \cdot \frac{1}{Re} \cdot (\nabla \cdot u) I \right] + F \\ \nabla \cdot (\rho u) = 0 \end{cases}$$

Navier-Stokes equation can be written in following form:

$$\begin{cases} \rho\frac{\partial u}{\partial t} + \rho(u\cdot\nabla)u = -\nabla p + \nabla(\mu(\nabla u + (\nabla u)^T) - \frac{2}{3}\mu(\nabla\cdot u)I + F \\ \frac{\partial \rho}{\partial t} + \nabla\cdot(\rho u) = 0 \end{cases}$$

where:

- $\rho\frac{\partial u}{\partial t} + \rho(u\cdot\nabla)u -$ inertial forces,
- $-\nabla p$ – pressure forces,
- $\nabla(\mu(\nabla u + (\nabla u)^T) - \frac{2}{3}\mu(\nabla\cdot u)I -$ viscous forces,
- F – external forces applied to the fluid,
- $\frac{\partial \rho}{\partial t} + \nabla\cdot(\rho u) = 0$ - continuity equation.

Non-dimensionalization of model is popular not only in fluid mechanics. Below are presented the other non-dimensional numbers:

Peclet number	$Pe = \frac{v_0 L_0}{\kappa}$	$\frac{convection}{diffusion}$	Used in calculations involving convective heat transfer,
Mach number	$M = \frac{\|v\|}{c}$		Indicate the speed of sound,
Prandtl number	$Pr = \frac{\mu}{\rho\kappa}$		Used in calculations of heat transfer between a moving fluid and a solid body.

5. SIMILARITY OF FLOWS

Linear Stock equations are characterized by specific symmetries, where the most important is symmetry with respect to time reversal.

Describing the Navier-Stokes equation

$$\begin{cases} \rho \dfrac{\partial v}{\partial t} + \rho(\vec{v} \cdot \nabla)\, \vec{v} = -\nabla \rho + \mu \Delta\, \vec{v} + F \\ \nabla \cdot \vec{v} = 0 \end{cases}$$

in non-dimensional units one can receive:

$$\begin{cases} \dfrac{\partial \vec{v}^*}{\partial\, t^*} + \left(\vec{v}^* + \nabla\right) \vec{v}^* = -\nabla^* \rho^* + \dfrac{1}{Re} \Delta\, \vec{v}^* + \vec{F}^* \\ \nabla \cdot \vec{v}^* = 0 \end{cases}.$$

The solution of equation is the same for the same Reynolds number, if the boundary condition expressed in non-dimensional variables are the same. The Reynolds number is the only ratio in this equation. It is called a number of similarities.

The flows are identical if they have the same geometry and Reynolds number, with units accuracy. It allows to the scaling of model whose dimensions are too big or too small, and subjected it to the tests, which will result in the correct values.

We can distinguish three types of similarities. First is the similarity of geometry which requires that real object and model object were geometrically similar. The similarity of kinematic postulates similarity of velocity fields in the flow in the real object and the object model. Dynamic similarity postulates similarity field forces acting on the real object and the object model.

Obtaining full similarity allows for simple conversion of the corresponding size of the model scale to the real scale – non-dimensional coefficients of forces and speeds are the same.

6. MATHEMATICAL DESCRIPTION OF MODEL 1

Model 2D was created in COMSOL Multiphysics by specifying coordinates of primitives and its necessary transformation.

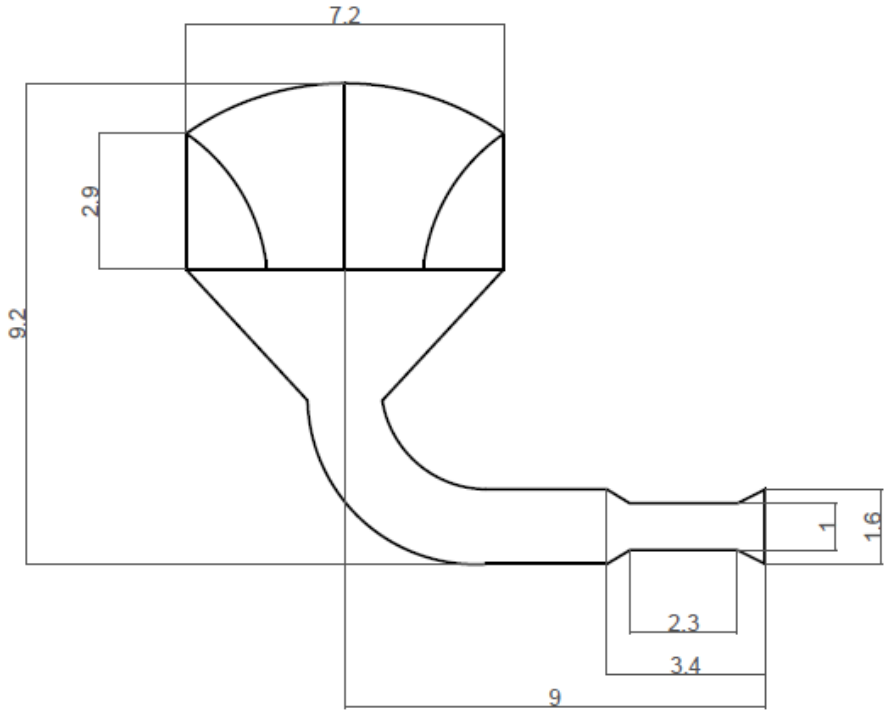

Figure 6.1 - Scaled dimensions of system

Model is the core element of conducted simulation. On the walls of the model the boundary conditions are imposed and they affect on the correctness of the carried out simulation. In this case, the calculation of model the real dimensions turned out impossible, therefore the model was scaled and one dimension, the diameter of Venturi section, was chosen as a basic one and its equal 1.

7. SIMULATION METHODOLOGY OF MODEL 1

First step of simulation was the determination of parameters. The speed of wind was defined as characteristic and it is equal 1. This value was defines as *U_wind*. After scaling in basic model the Length of Venturi is equal 3.6. It is possible to change this parameters by changing the value in window (Figure 5.1).

Name	Expression	Value	Description
D	1	1	Diameter of Venturi
L	3.4	3.4	Length of Venturi
U_wind	1	1	Speed of Wind
rho	1.23	1.23	Density of Air
ni	3e-5	3.0000E-5	Viscosity
Re	U_wind*D*rho/ni	41000	Reynolds Number
Rem1	1/Re	2.4390E-5	
Repar	1	1	
U_wind2	0.1	0.1	Speed of Winf on Inlet 1

Figure 7.1 - Window of parameters

By *ni* the value of the viscosity of air is determined. The Reynolds number is calculated from the formula:

$$Re = U_{wind} \cdot D_v \cdot \frac{rho}{ni}.$$

Second step was to create a model. The closed contour of INVELOX was changed into solid.

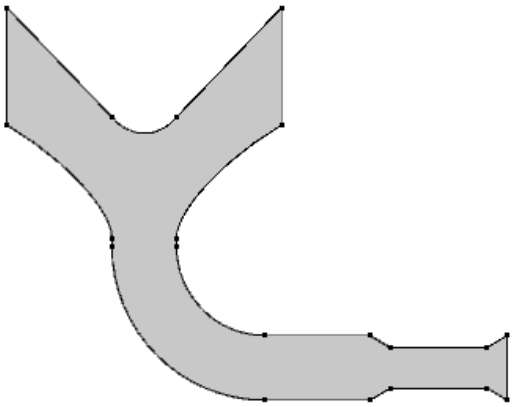

Figure 7.2 - Geometry of INVELOX generated in COMSOL

The third step is selection of a material. The COMSOL library consists of different kinds of material like liquid and gases, Bioheat, Nonlinear magnetic etc.

The Air was chosen with follow parameters. The model is non-dimensional then the density is 1 $\frac{kg}{m^3}$ and the dynamic viscosity is equals $\frac{1}{Re_{par}}$ $Pa \cdot s$ what is also 1.

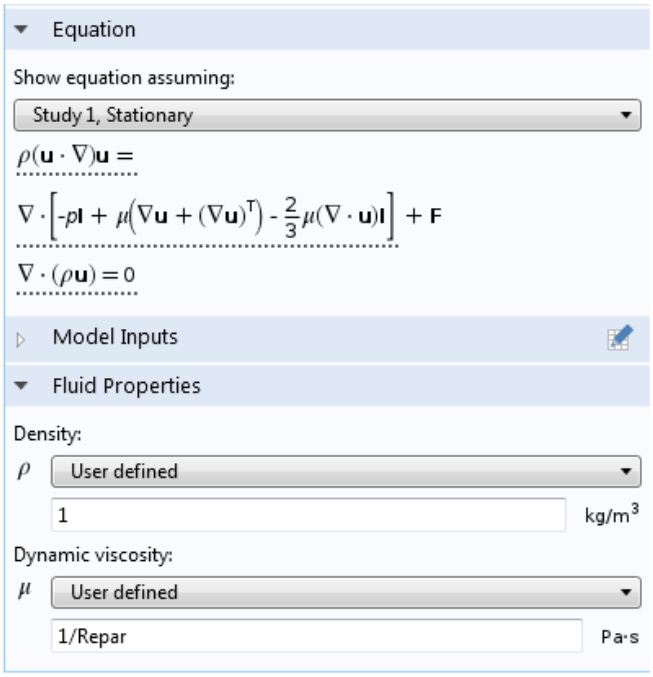

Figure 7.3 - Fluid parameters

The most important is a correct determination of boundary condition. As is showed on Figure 5.5 two walls was chosen as a inlets. The wind speed in inlet one (1) is equal 1. The INVELOX is omnidirectional system what means that the wind enters from every direction. Therefore, in the second inlet (2) these value is declared as velocity field equal in direction x and z axes 0. Both, the wall number 2 and number 3 was declared as outlet. The boundary parameter in wall 3 was the pressure condition. The pressure is equals 0 Pa.

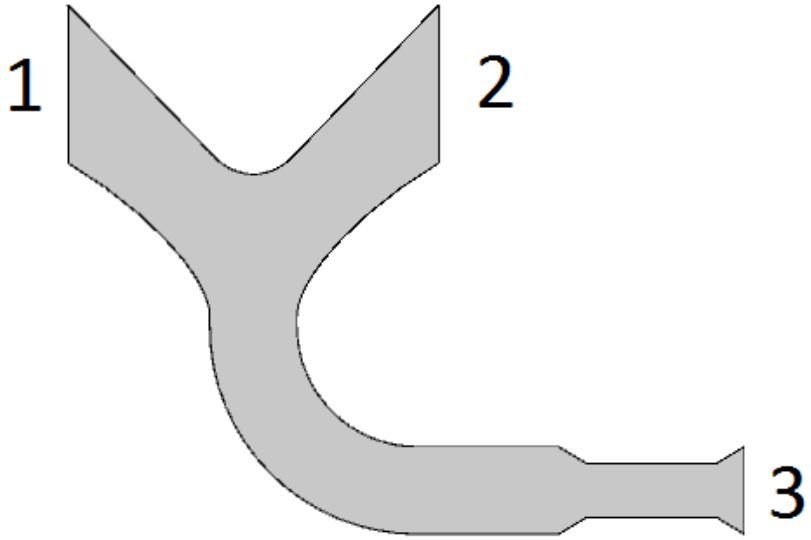

Figure 7.4 - Defined walls

The boundary condition on the rest of wall assumes no slip on these walls.

Following step is creation of mesh. The size of mash has a giant influence on the process of the simulation. If the mesh will be too large the calculation of flow in too narrow Venturi section may be impossible.

The element size was calibrated for fluid dynamics and the fine sized mesh was used.

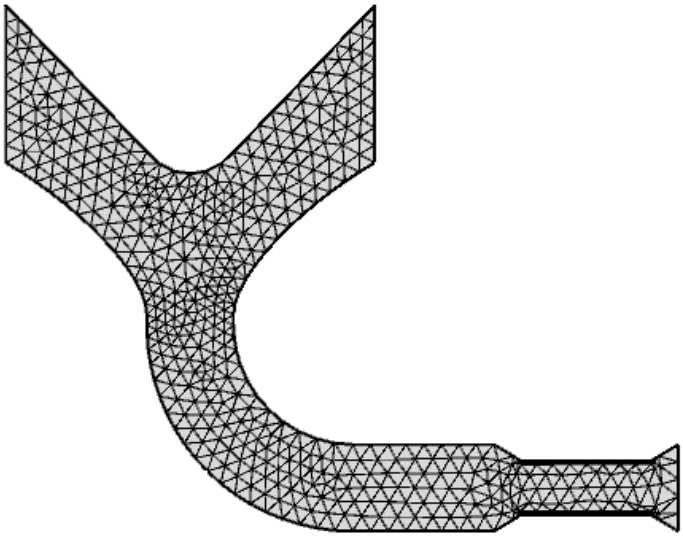

Figure 7.5 - Model with mesh

Additionally on two walls of Venturi the four boundary layers with stretching factor equal 1.2 was added.

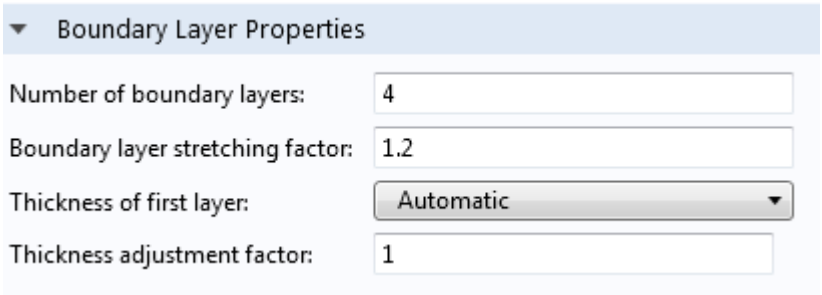

Figure 7.6 - Condition of boundary layers

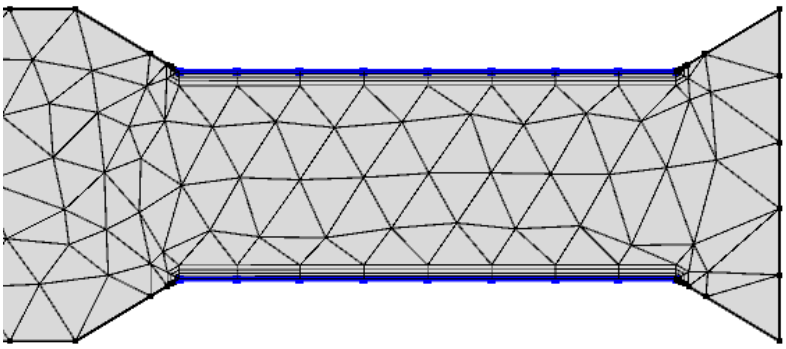

Figure 7.7 - Boundary layers conditions

The last step was to determination of Parametric Sweep. The Reynolds Number will be equals from 10^0 up to 10^6

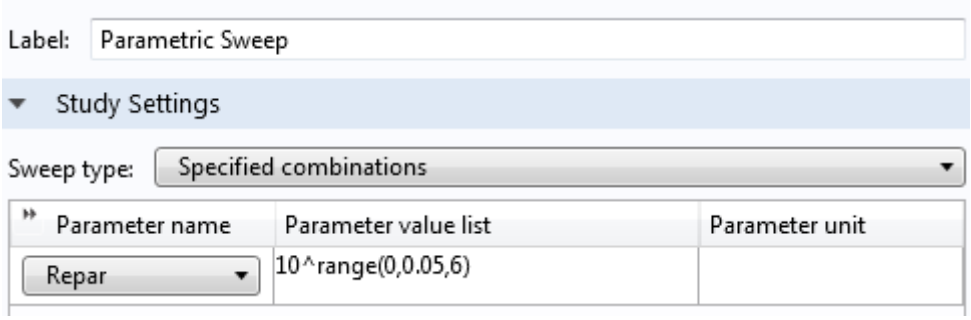

Figure 7.8 - Parametric sweep definition

8. RESULTS OF SIMULATION OF MODEL 1

8.1. Time independent study

Simulation was performed with different value of wind speed at the both inlets.

The first case assumed that a wind is able to blow from one direction only. The speed of wind at the Inlet 1 was equals 0.9 and at the second one 0.1.

8.1.1. Parameters of inlets velocities: U_wind=0.9, U_wind2=0.1

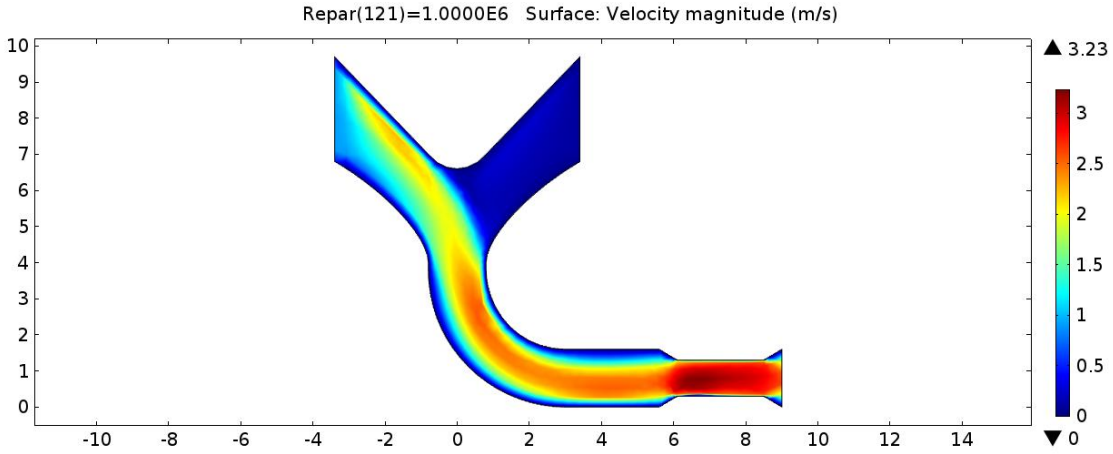

Figure 8.1 - Velocity field for Repar parameter equals 1 million

Figure 8.1. shows velocity field. As we cans see in the Venturi section the highest value of velocity is equal 3.23. That means that the wind which blows from one direction has been increased its speed about 3 times.

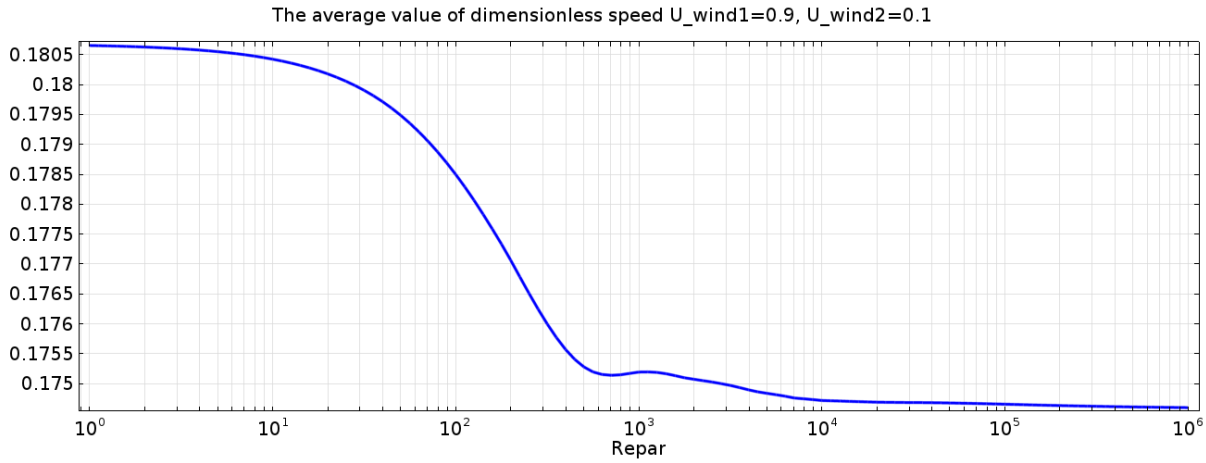

Figure 8.2 - Dependence of Reynolds numbers to wind speed

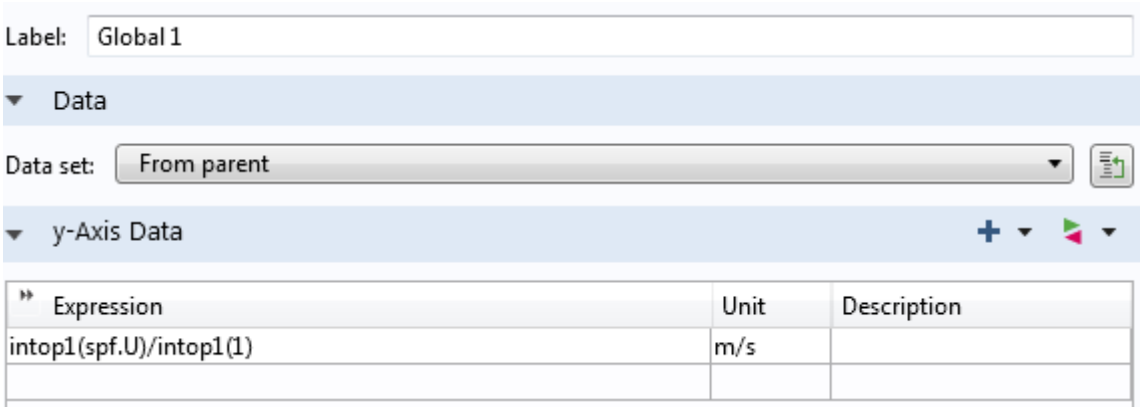

Figure 8.3 - Setting window

Setting window 8.3 shows how the equation was changed in program.

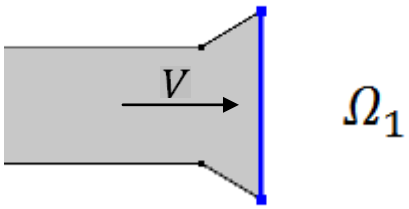

Figure 8.4 - The average velocity at the outlet

COMSOL expression of mean value of magnitude of velocity at inlet boundary:

$$\overline{|\mathrm{v}|} = intop1(spf.U)/intop1(1)$$

can be written as:

$$\overline{|\mathrm{v}|} = \frac{\int_{\Omega_1} |\mathrm{v}| d\Omega_1}{\int_{\Omega_1} d\Omega_1}$$

where $\overline{|\mathrm{v}|}$ is a average speed of wind at the inlet.

For the laminar flow when the layers of fluid are in close contact with the submerged object, we can expect high viscous, and therefore, the ratio of inertia force forces and viscosity (Reynolds number) will be small.

During the turbulent flow, the presence of eddies will result in no ideal flow around a submerged body. We can expect higher inertia forces (impact of the liquid on the surface of the object). Ratio of the forces of inertia and viscosity forces will be a large number because the viscous forces are small and the inertia increases together with higher flow rate.

The smaller Reynolds numbers say that these objects interact with the air to a greater extent with a viscosity forces than a forces of inertia.

As we can observe at the diagram 8.2. the wind speed is decreasing together with increase of Reynolds number. That means that the values of inertia forces is higher than viscosity forces. This ratio increases together with decreasing of wind speed.

If we assume the average wind speed of whole model area we need to change the expression:

$$\overline{|\mathrm{v}|} = \frac{intop2(spf.U)}{intop2(1)}$$

and it is equivalent to the equation:

$$\overline{|\mathrm{v}|} = \frac{\int_{\Omega} |\mathrm{v}| d\Omega}{\int_{\Omega} d\Omega}.$$

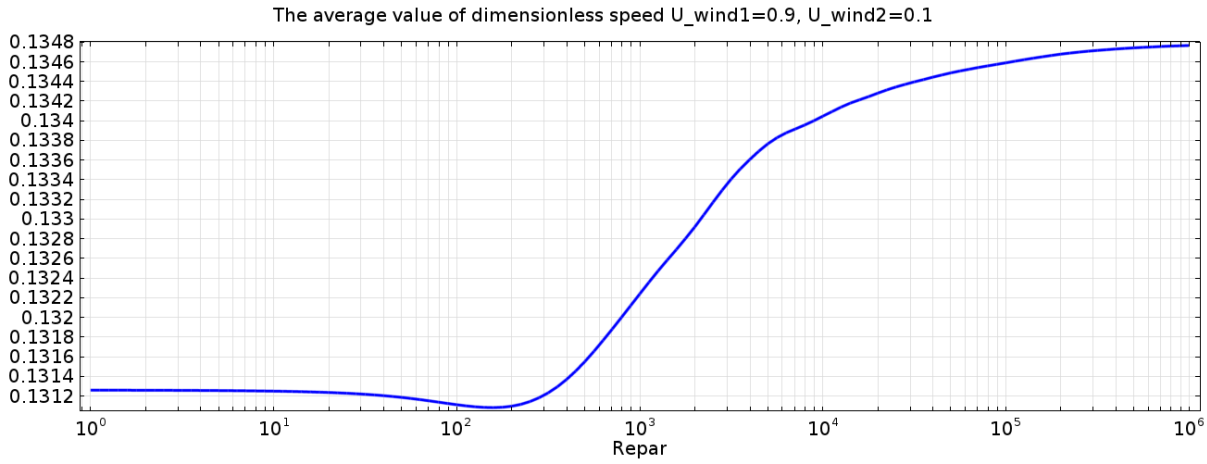

Figure 8.5 - Increasing value of Reynolds number together with the average value of dimensionless speed

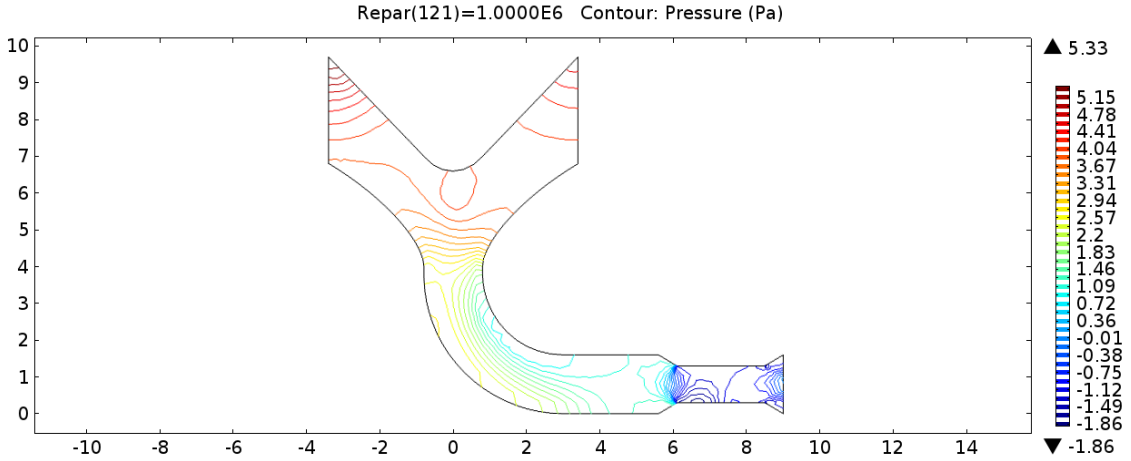

Figure 8.6 - Distribution of pressure

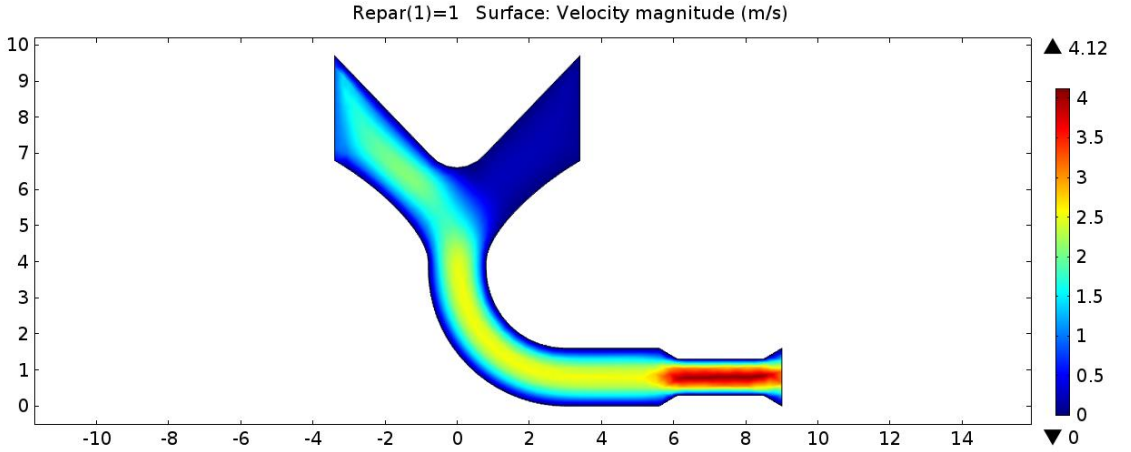

Figure 8.7 - Distribution of velocity magnitude for Repar parameter equals 1

Decreasing of Reynolds number caused a increasing of wind velocity in crucial Venturi section up to 4.12.

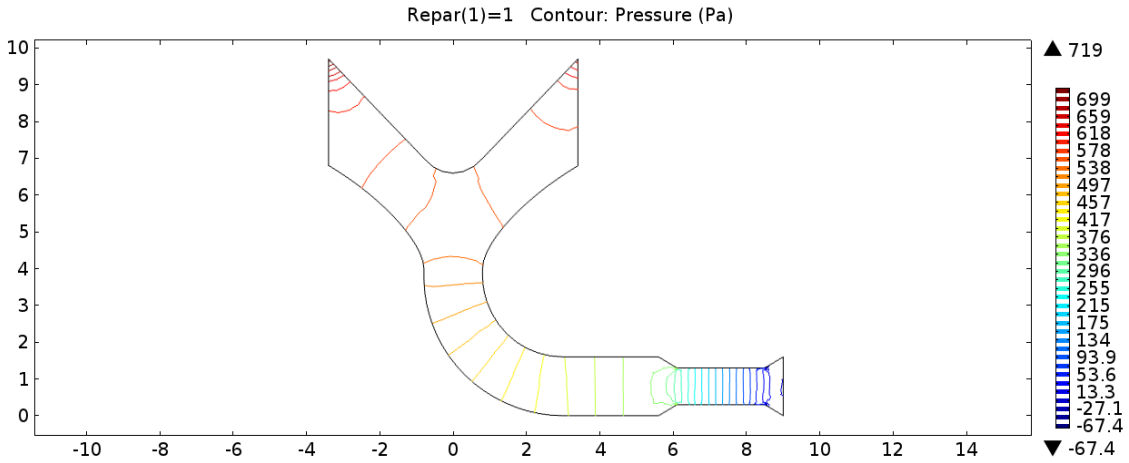

Figure 8.8 - Distribution of pressure

8.1.2. Parameters of inlets velocities: U_wind=0.1, U_wind2=0.9.

In second case the wind blowing from opposite direction is assumed. Value of wind speed at the first inlet is equal 0.1, and at the second one 0.9.

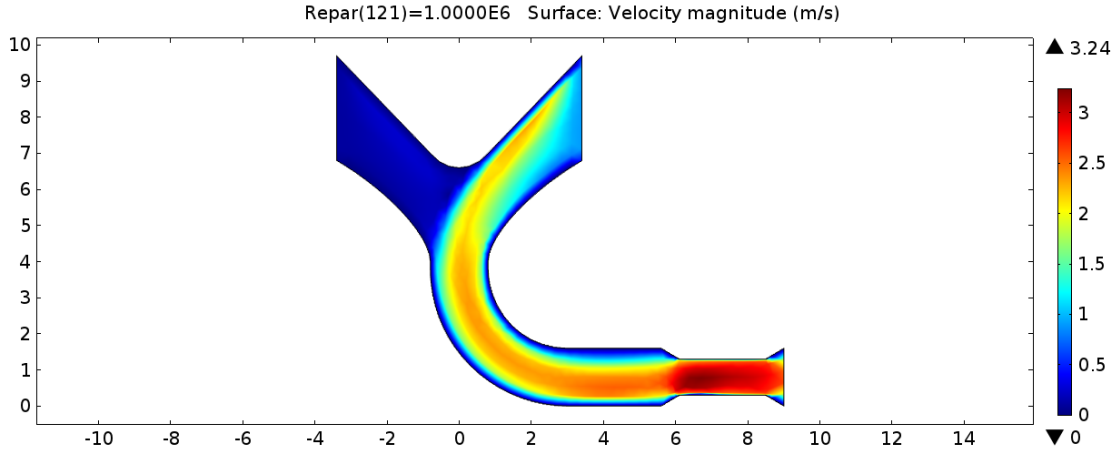

Figure 8.9 - Velocity field for Reynolds number equal 1 million

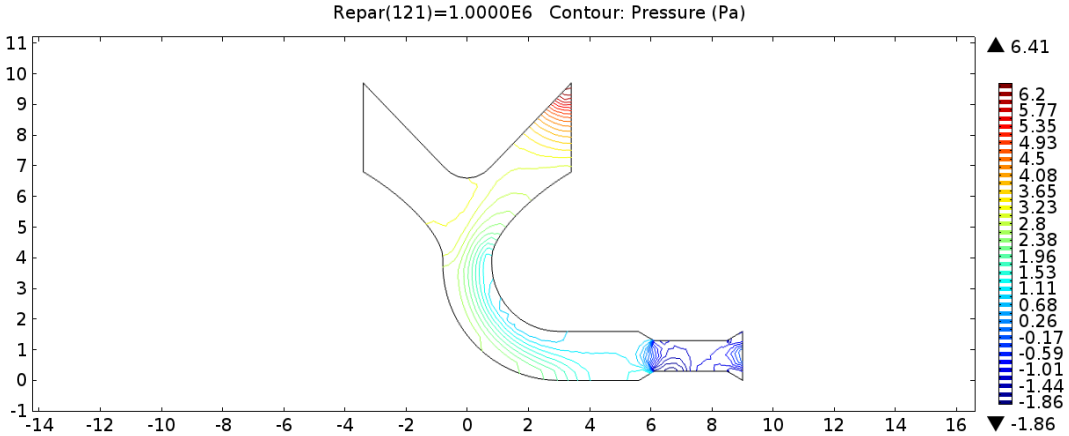

Figure 8.10 - Pressure distribution with the Reynolds number equals 1 million

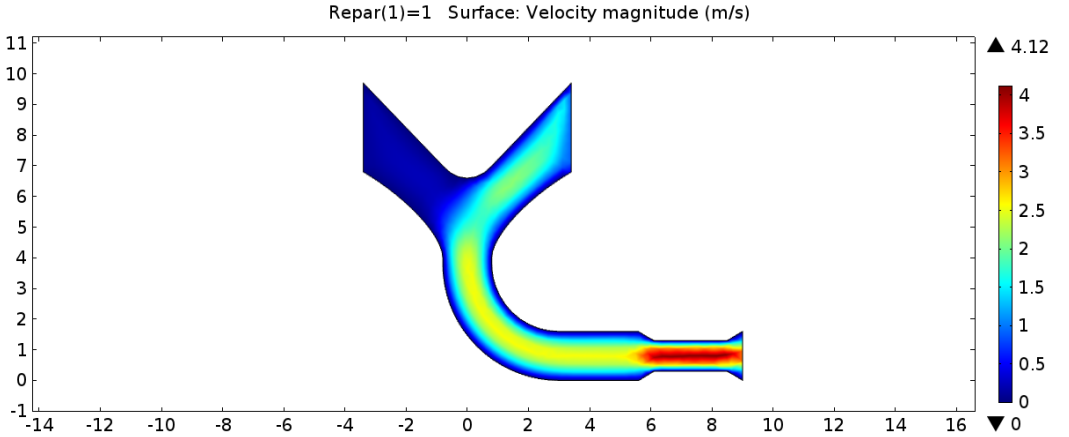

Figure 8.11 - of wind speed with Reynolds number = 1

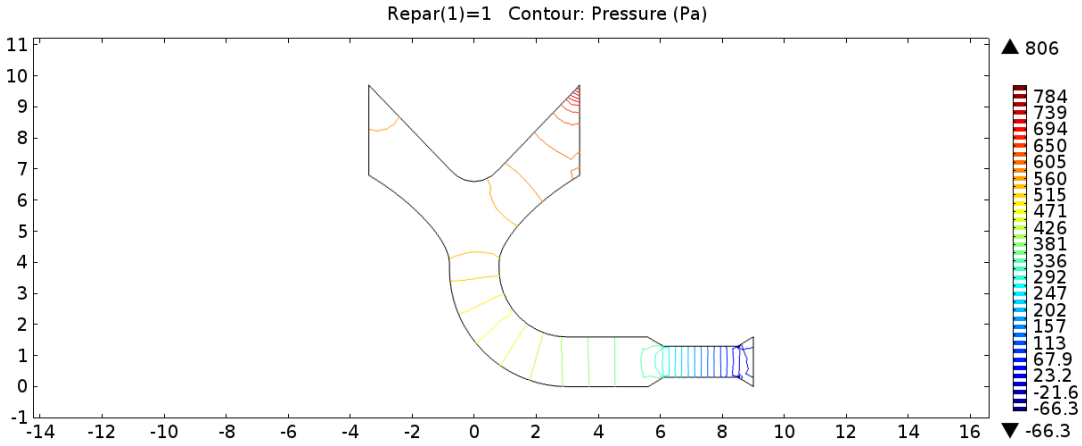

Figure 8.12 - Pressure distribution with Re = 1

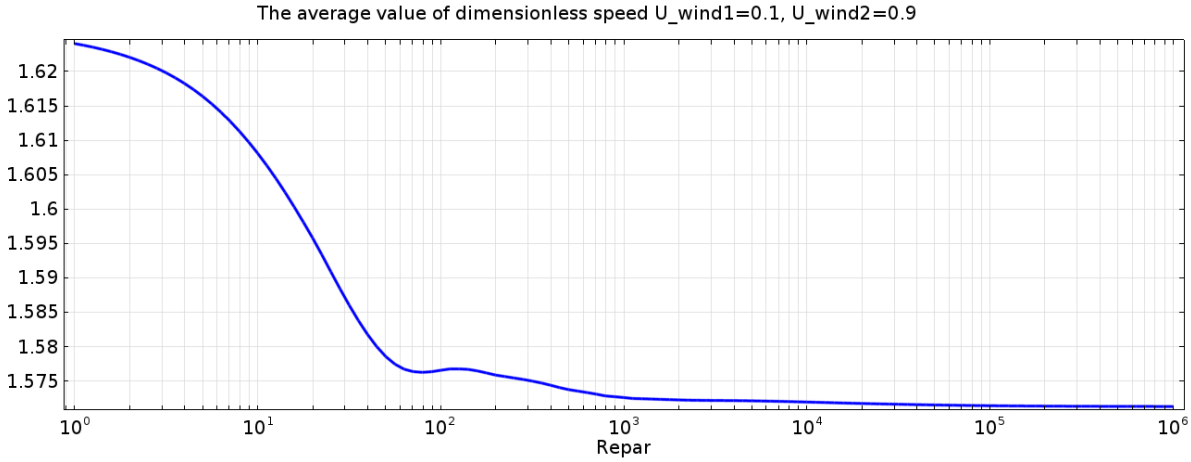

Figure 8.13 - Dependence of average wind velocity at the outlet on the Reynolds number

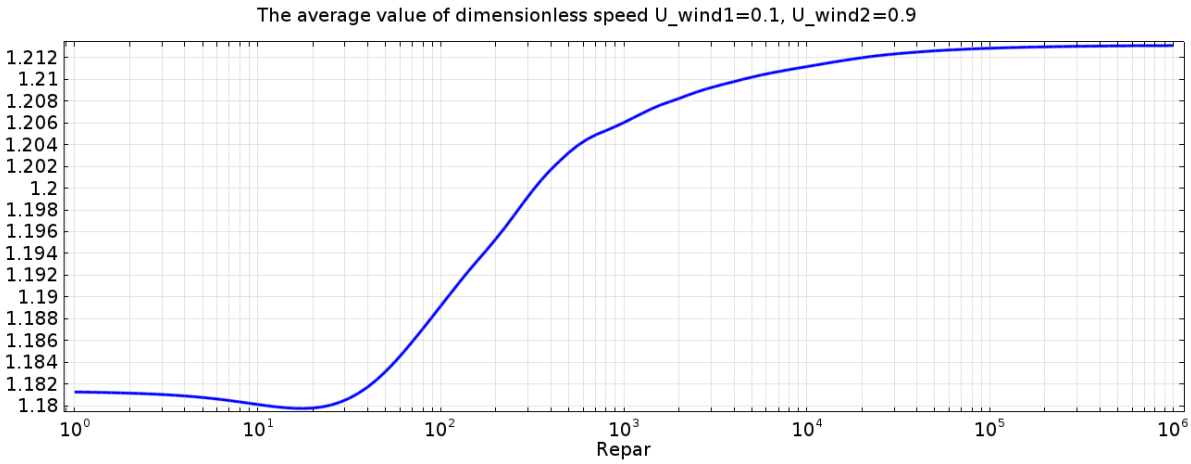

Figure 8.14 - Dependence of average wind velocity at the field of model on the Reynolds number

8.1.3. Parameters of inlets velocities: U_wind=0.6, U_wind2=0.4

Last case established that the wind speed values are nearly even and equal U_wind = 0.6, U_wind2 = 0.4. It is a possible use of omnidirectional INVELOX System. We assume wind blowing from two directions simultaneously.

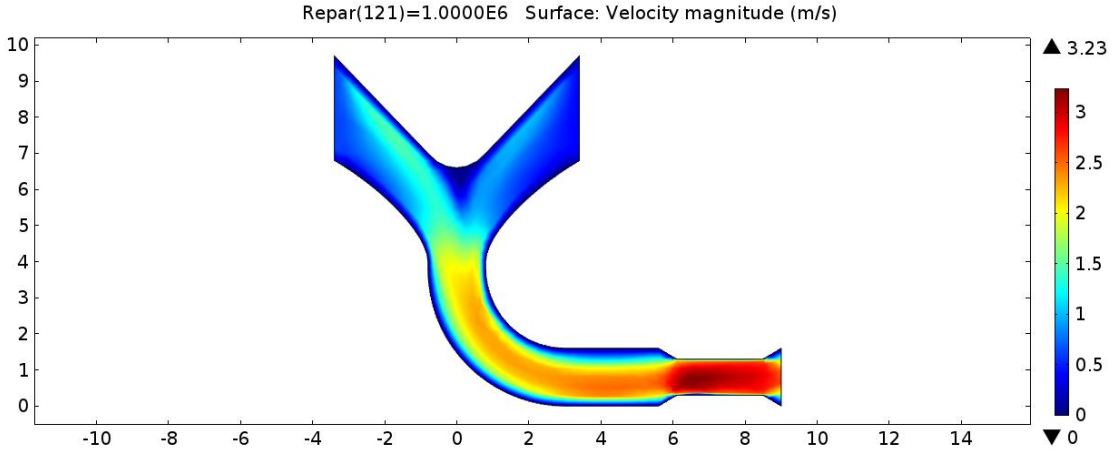

Figure 8.15 - Fields of velocity for Reynolds number equals 1 million

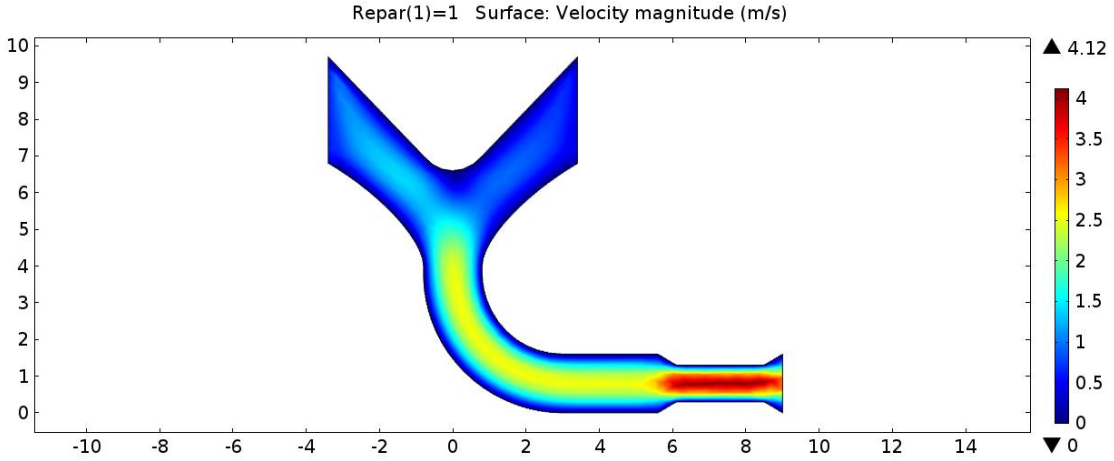

Figure 8.16 - Fields of velocity for Reynolds number equals 1

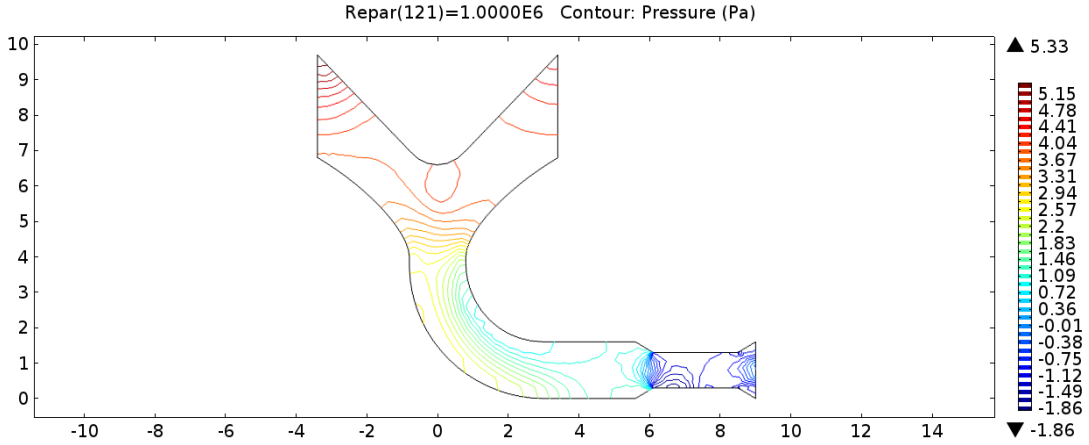

Figure 8.17 - Fields of pressure for Reynolds number equals 1

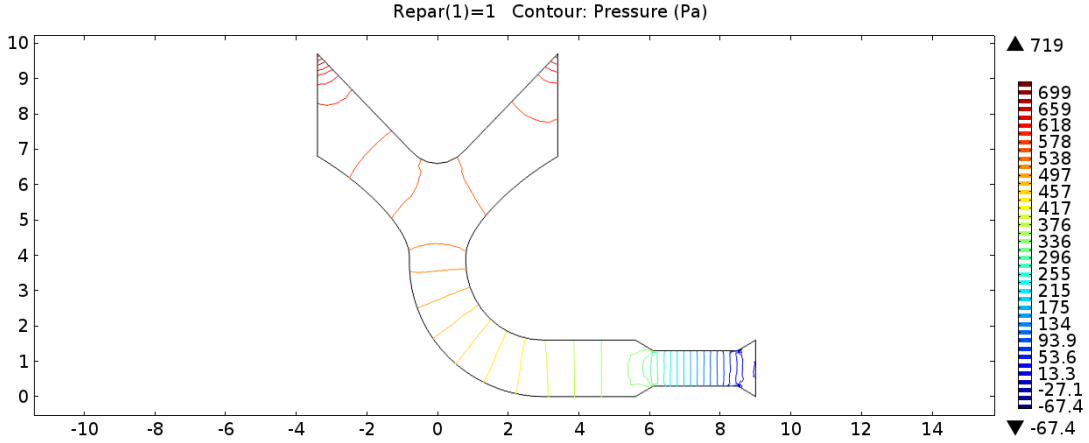

Figure 8.18 - of pressure for Reynolds number equals 1 million

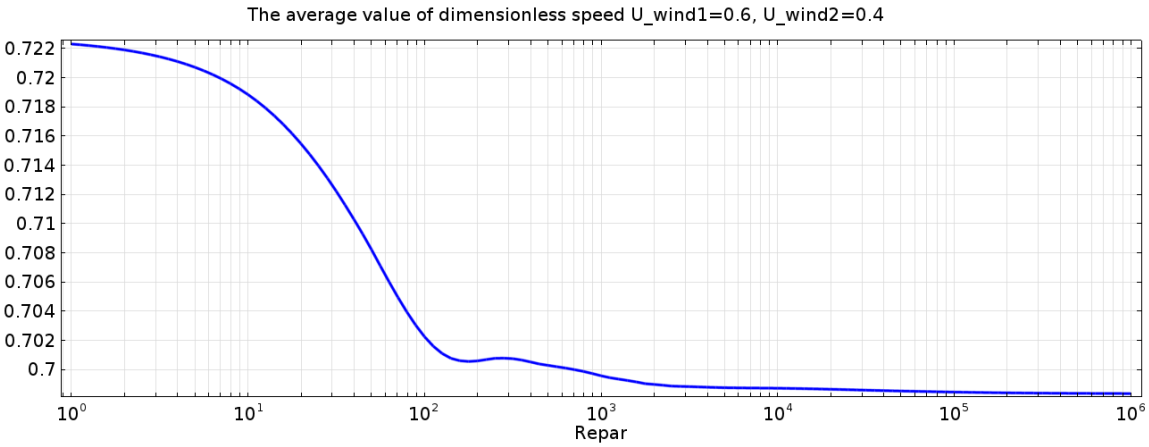

Figure 8.19 - Dependence of average speed velocity at the inlet on the model

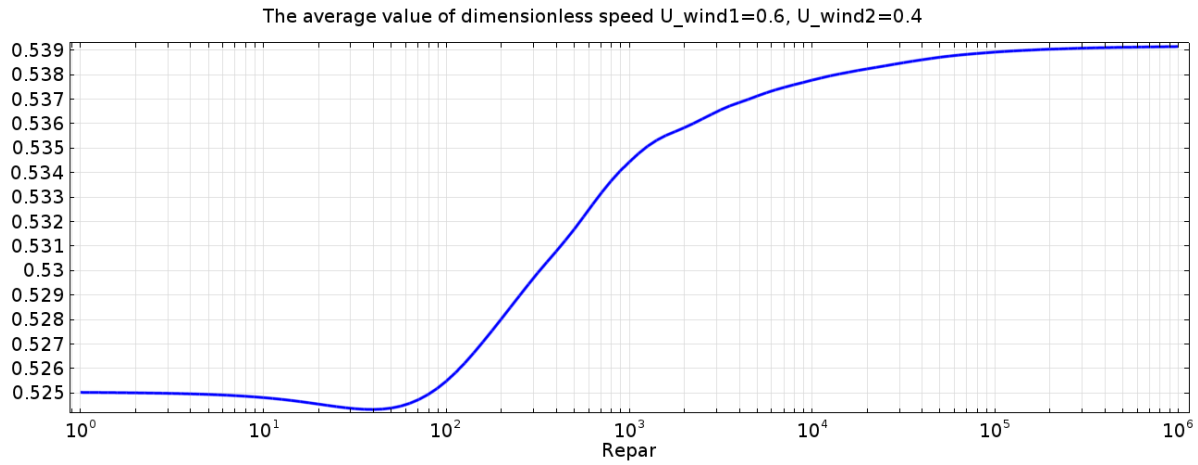

Figure 8.20 - Dependence of average wind velocity of model field on increasing Reynolds number

8.2. Time dependent study

The another step of simulation is to make conditional the velocity of wind on the time. It let us to show how field variables change over time. In fluid mechanics it is used to compute unsteady flow and pressure fields.

To perform this kind of simulation another study in COMSOL was defined.

At first, the wind velocity was dependent on time:

Figure 8.21 - Dependence of the speed of the time

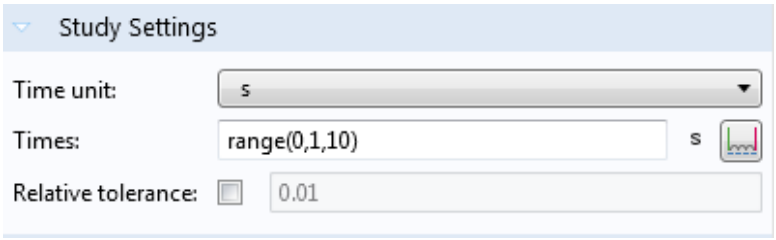

Figure 8.22 - Declaration of time range of simulation

As initial conditions for unsteady flow has been chosen solution for stationary flow for a given Reynolds number (Repar). In this case Repar is equals 100.

8.2.1. Results of simulation

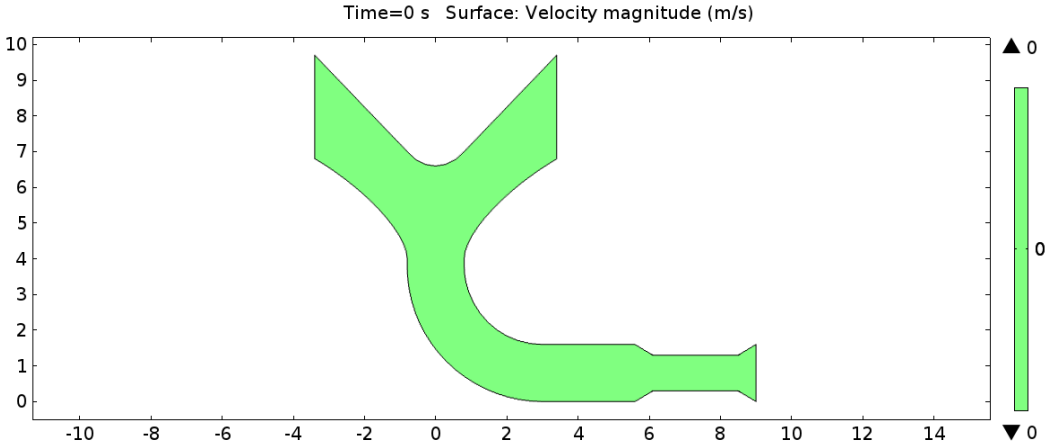

Figure 8.23 - Result of flow simulation in 0s

At the beginning of simulation the wind speed is equal 0, so any flow is existed. At the pictures 8.15a-8.15k the changes of velocity field are presented.

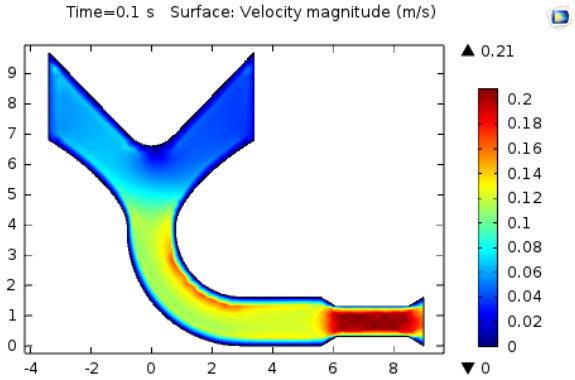

Figure 8.24 - 0.1 s

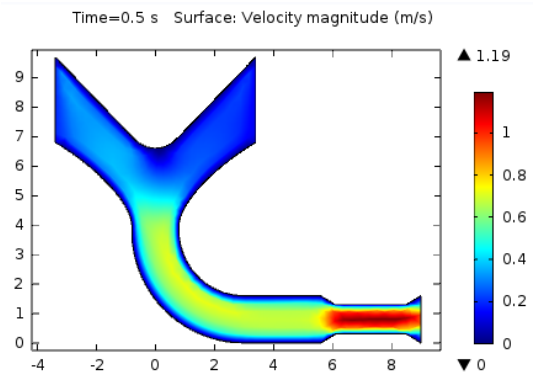

Figure 8.25 - 0.5s

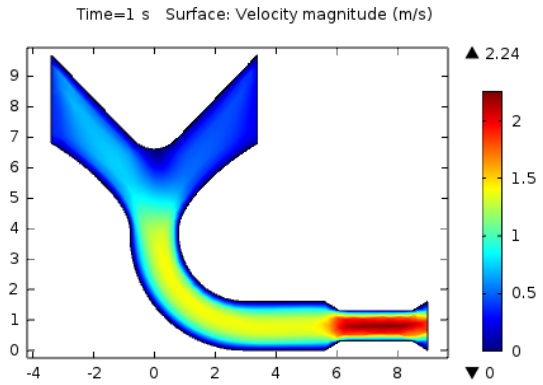

Figure 8.26 - 1s

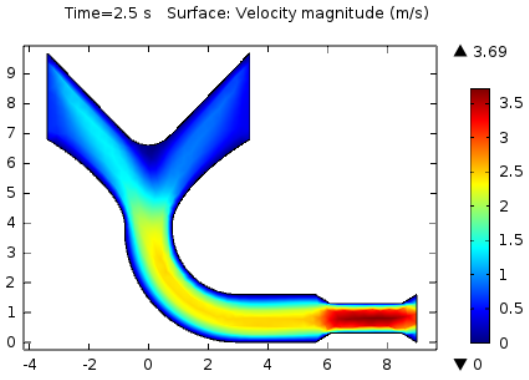

Figure 8.27 - 2.5 s

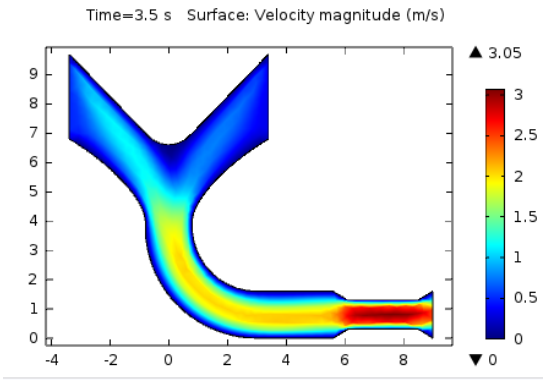

Figure 8.28 - 3.5 s

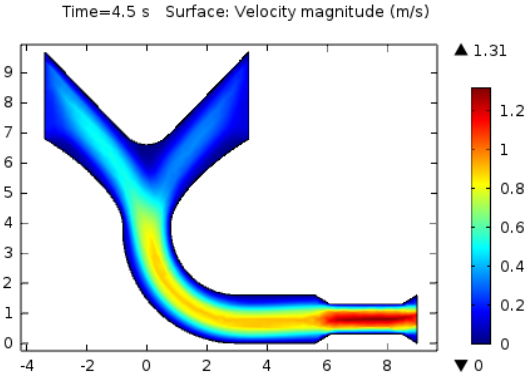

Figure 8.29 – 4.5 s

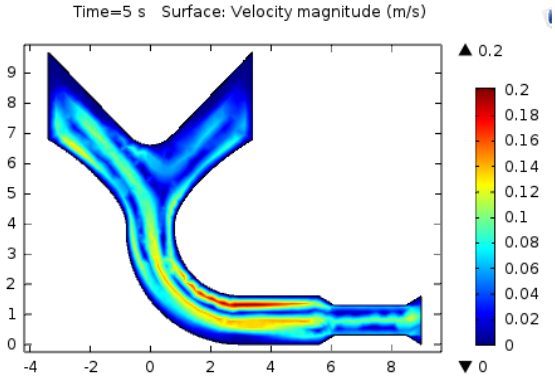

Figure 8.30 - 5 s

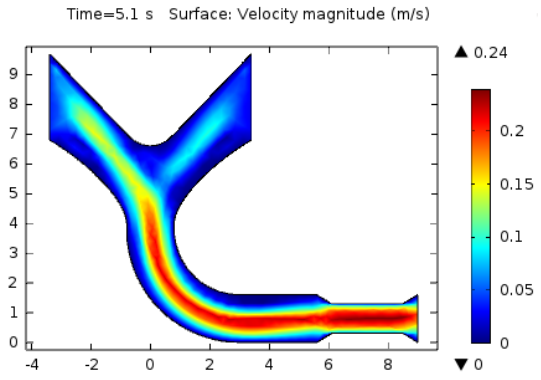

Figure 8.31 - 5.1 s

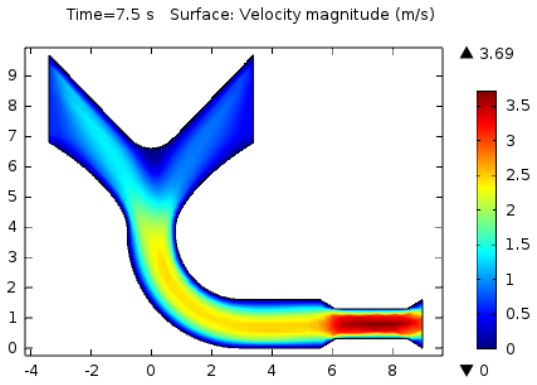

Figure 8.32 - 7.5 s

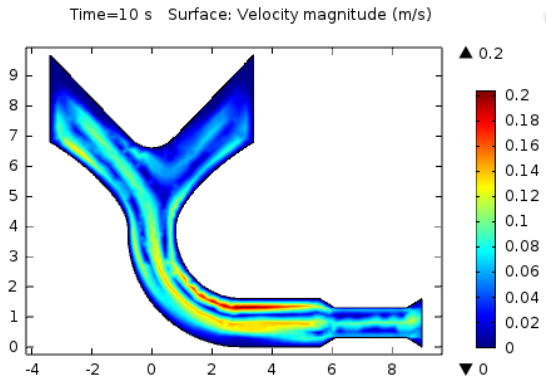

Figure 8.33 - 10 s

As we can see the highest value of velocity is received in 2.5th second and 7.5th second. The lowest one is in 5th second and 10th seconds.

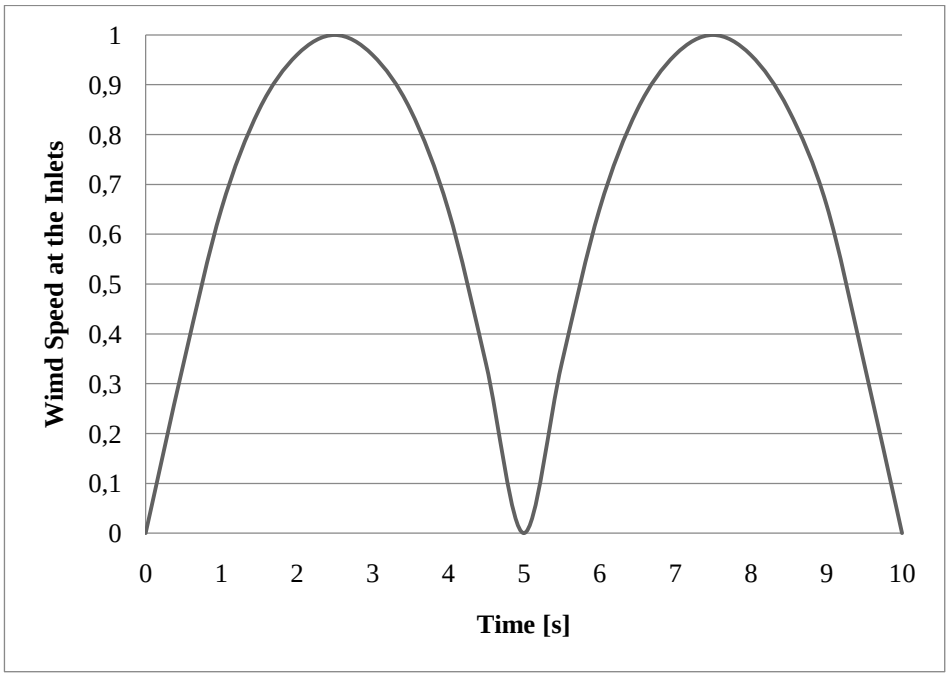

Figure 8.34 - Graph of velocity of wind at inlets to structure distribution

At the graph 8.34. we can observe a distribution of wind speed at the inlets during 10 s.

9. MATHEMATICAL DESCRIPTION OF MODEL 2

Model 2 is a one directional tube with wider diameter of inlet that the outlet. The diameter of inlet [fig. 9.2.] is equals 5.5 m. The diameter of Venturi section and outlet are this same as in first case in Model 1 [fig.7.1.]. Total length of model is equals 11 m.

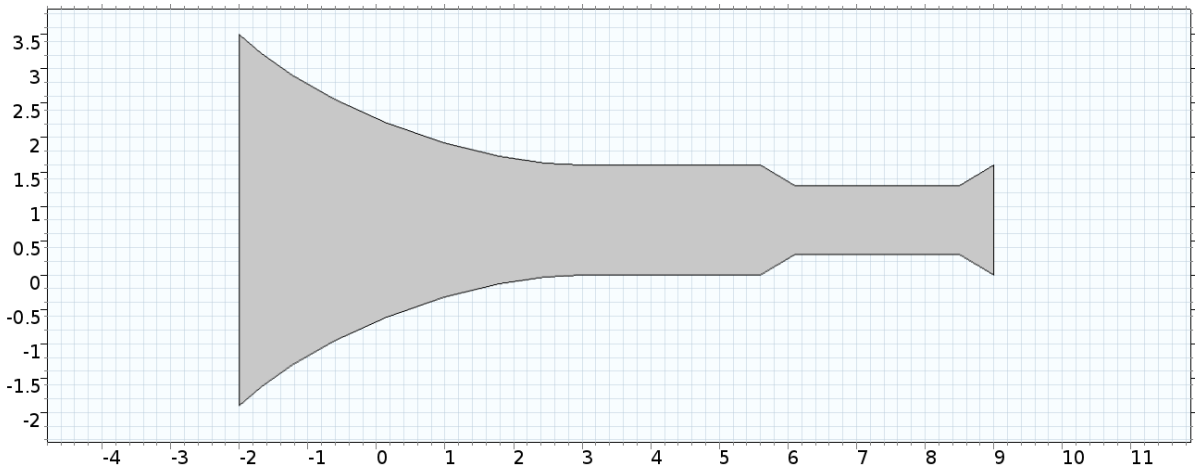

Figure 9.1 - Model 2 in COMSOL

The Wall 1 is defined as Inlet with wind speed 1. The wall 2 is an outlet.

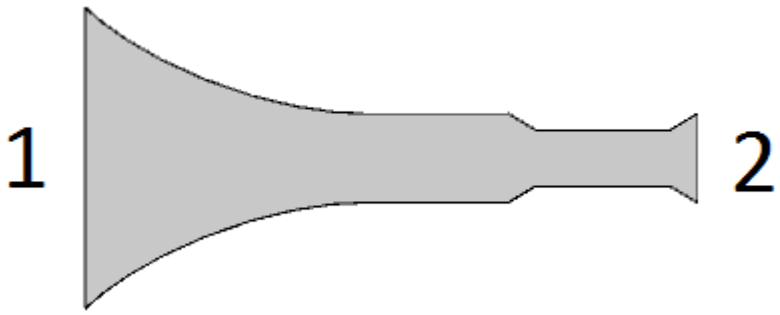

Figure 9.2 - Definition of Inlet 1 and Outlet 2

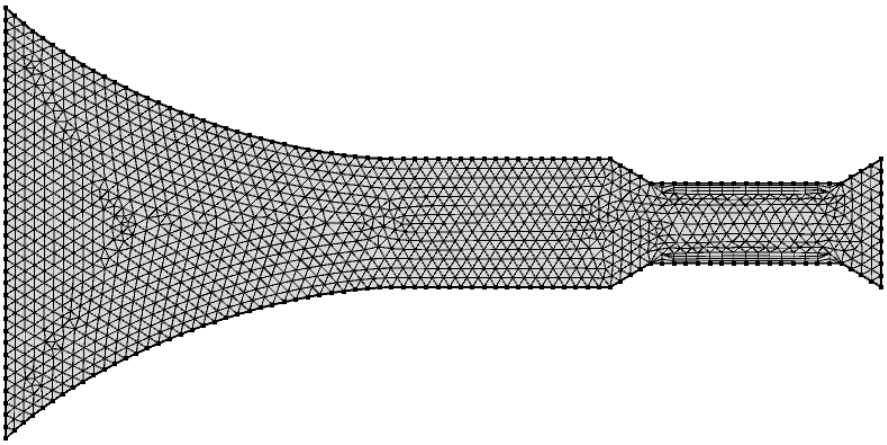

Figure 9.3 - Meshed element in COMSOL

Due to easier geometry of model 2 than model 1, the finer mesh was generated.

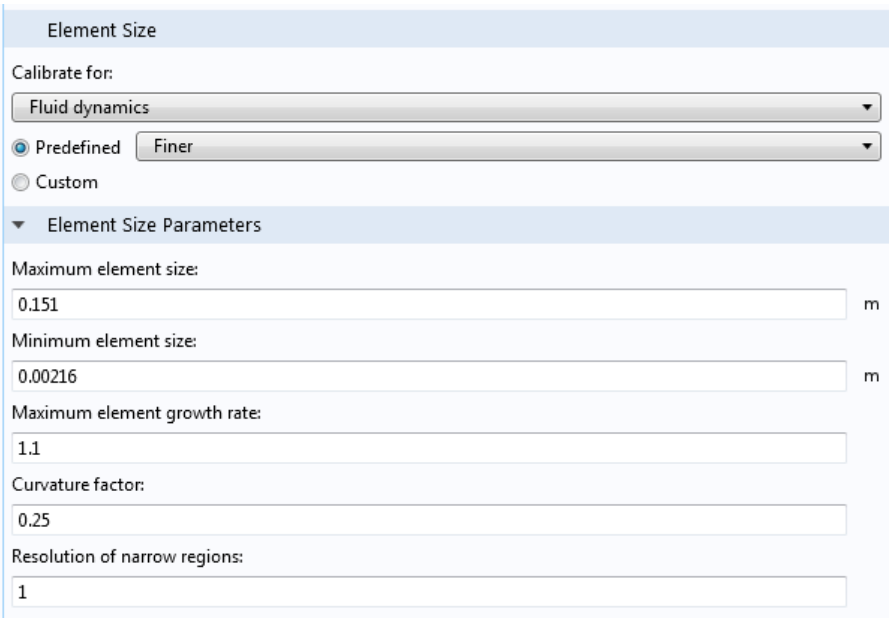

Figure 9.4 - Parameters of Mesh

The smallest element has size equals 2.16 mm. Reducing the geometry of the grid allows for more accurate performance calculations.

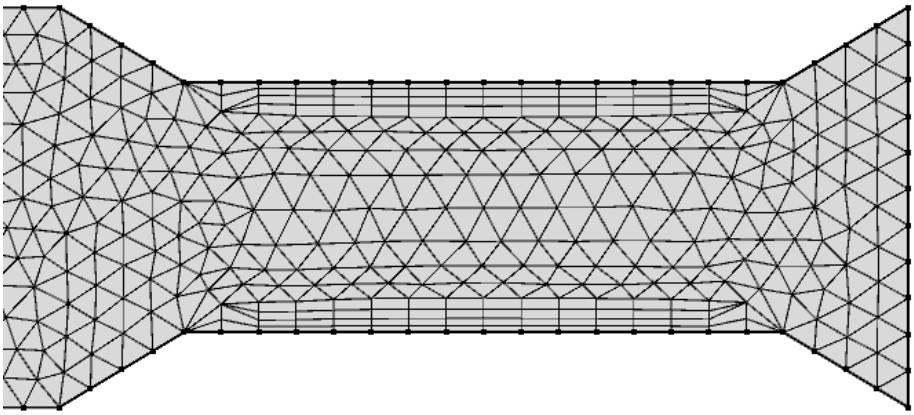

Figure 9.5 - Boundary layers of Venturi section in Model 2

As in the first case additional boundary layers properties has been applied in Venturi section. Four subsidiary layers was generated to accurately map the impact of the system on the flowing gas.

10. RESULTS OF SIMULATION OF MODEL 2

10.1. Time independent study.

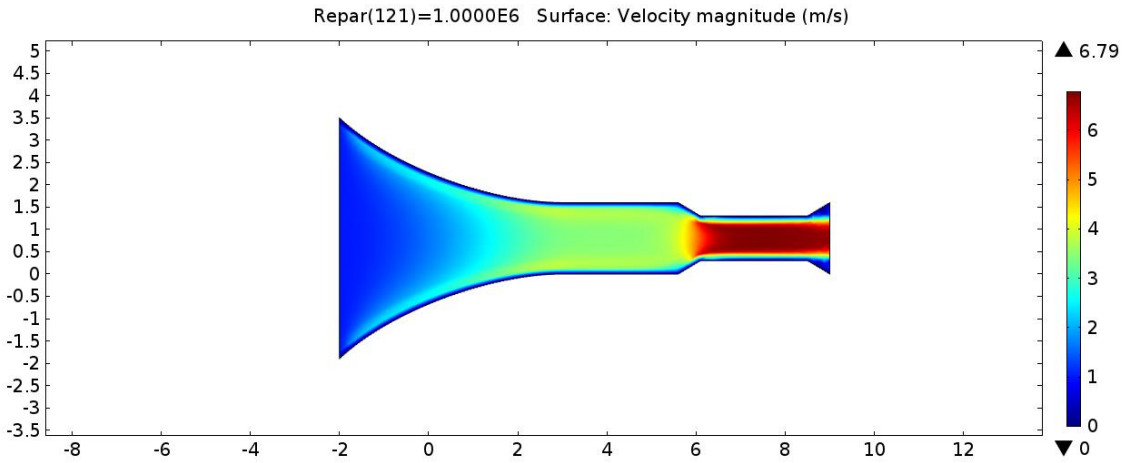

Figure 10.1 - Velocity magnitude for Reynolds number equals 1 million

According to the graph 10.1. the wind speed in Venturi increased up to 6.79. It is almost 7 times higher value than the value established at the inlet.

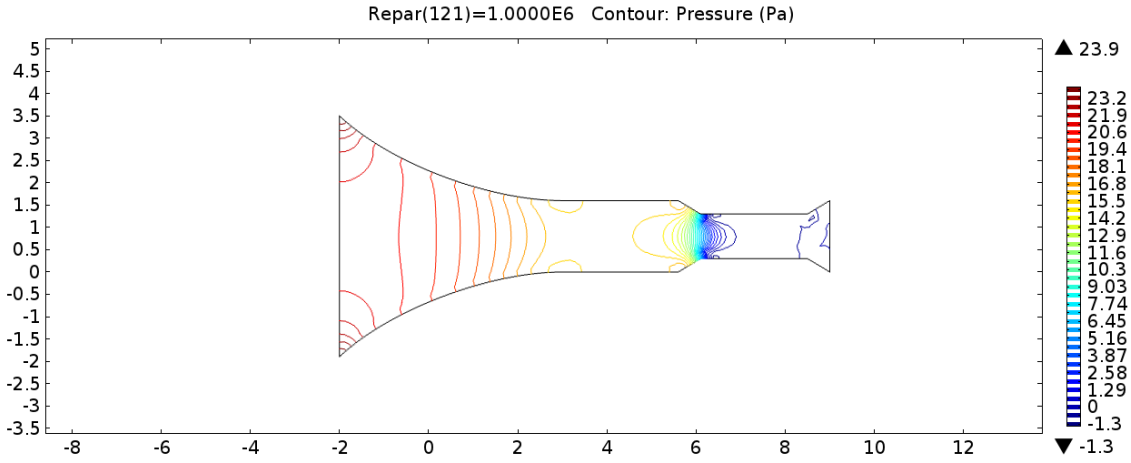

Figure 10.2 - Pressure magnitude for Reynolds number equal 1 million

The under-pressure which is shown in the above graph is a result of the assumptions adopted in simulation, and probably does not occur in the real model.

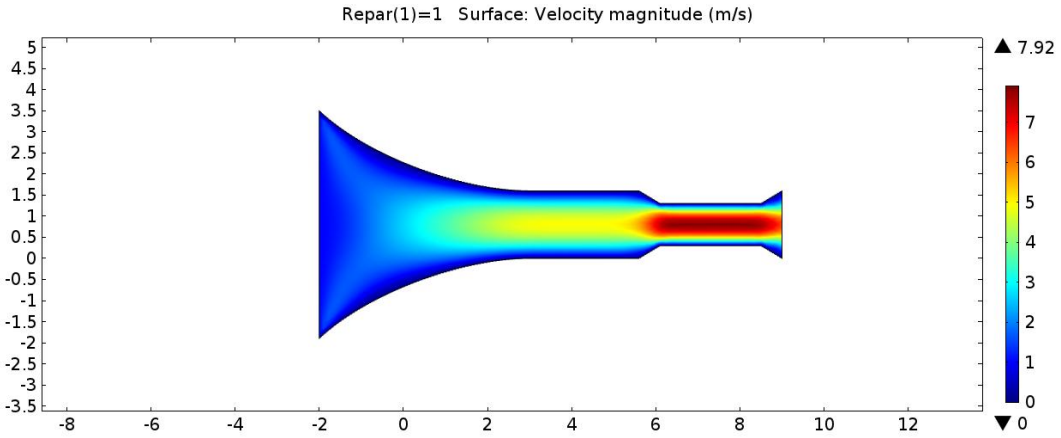

Figure 10.3 - Velocity fields for Reynolds number equals 1

10.2. Time dependent study

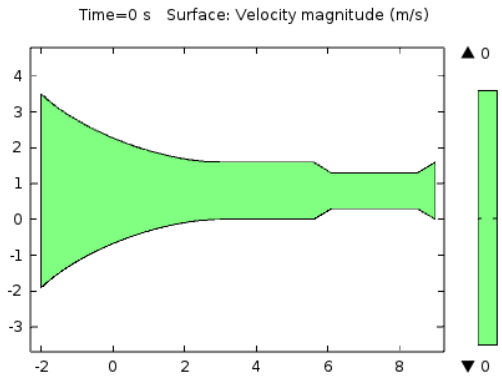

Figure 10.4 - 0 s

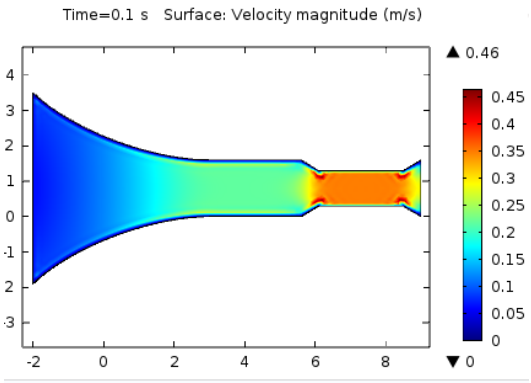

Figure 10.5 - 0.1 s

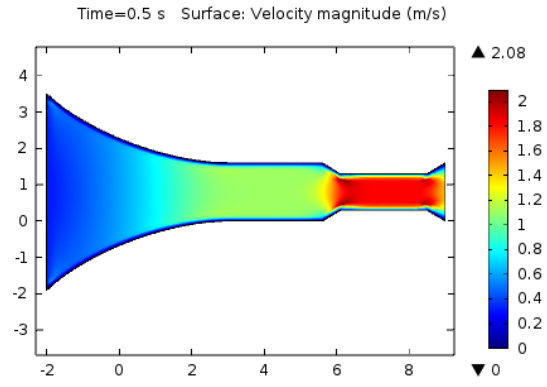

Figure 10.6

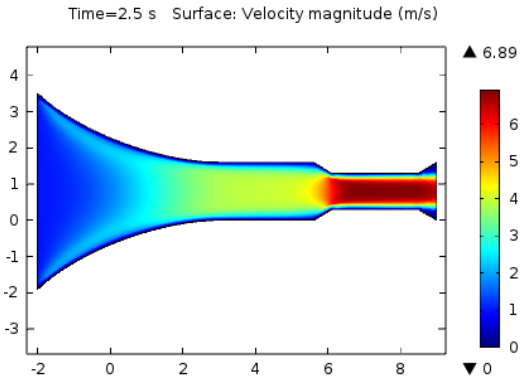

Figure 10.7 - 2.5 s

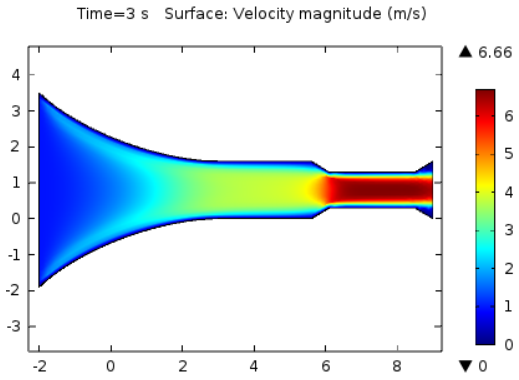

Figure 10.8 – 3 s

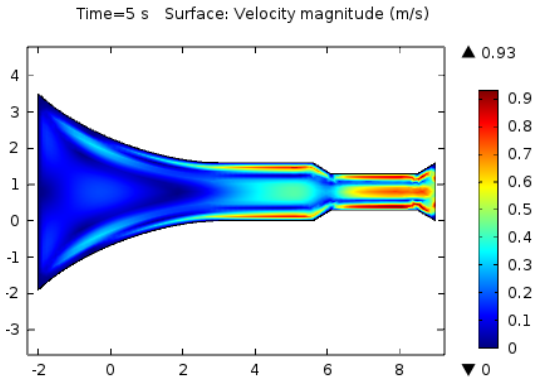

Figure 10.9 - 5 s

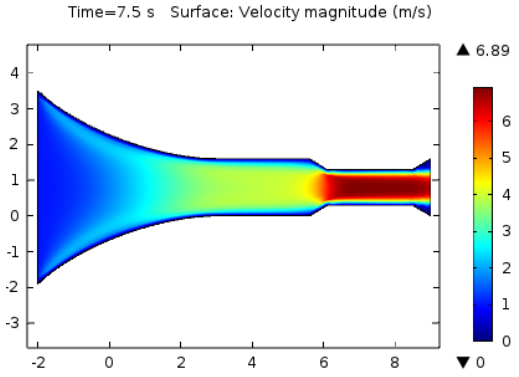

Figure 10.10 - 7.5 s

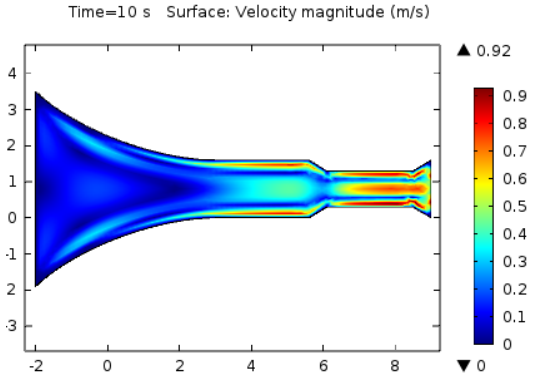

Figure 10.11 - 10 s

According to the above photos we can see that the highest value of wind speed is at 2.5th second and at 7.5th second.

11. COMPARISION OF RESULTS

Model 1

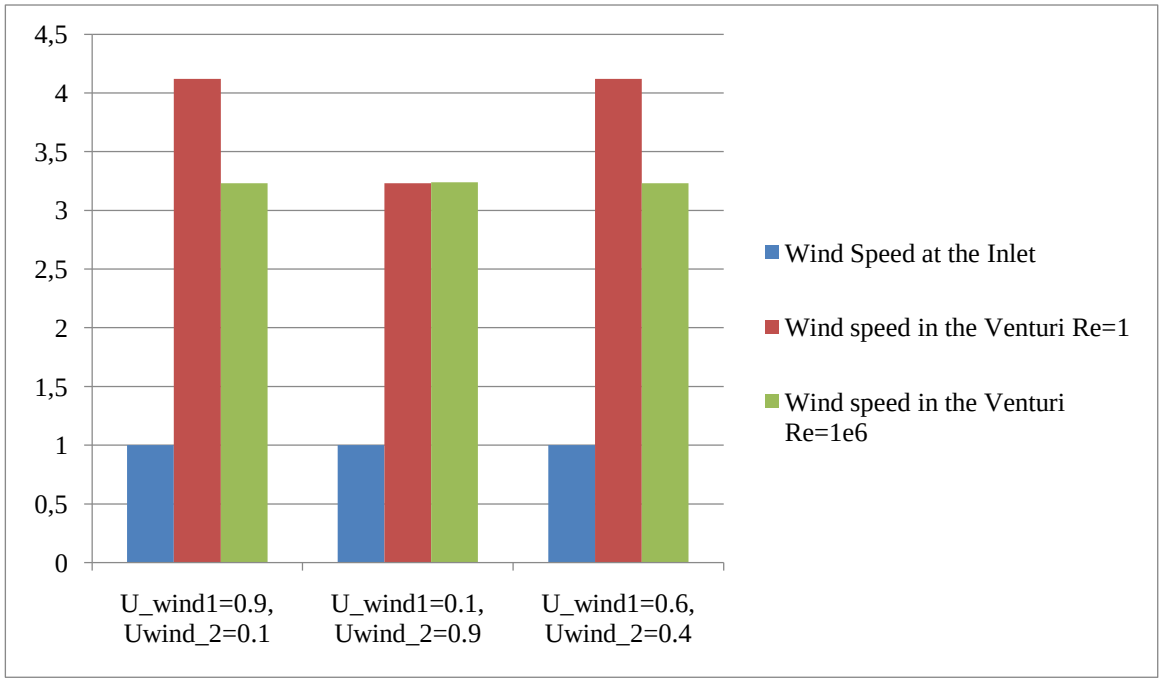

Figure 11.1 - Comparison of wind speed in Model 1at the inlet and outlets in dependence of Reynolds number

As we can observe at the diagram 11.1 the highest value of wind speed in Venturi is reached for first and last case of inlets speed assumptions and Reynolds number equal 1. It is equals 4.12, what means that the wind speed has increased more than 4 times in crucial part of system.

Model 2

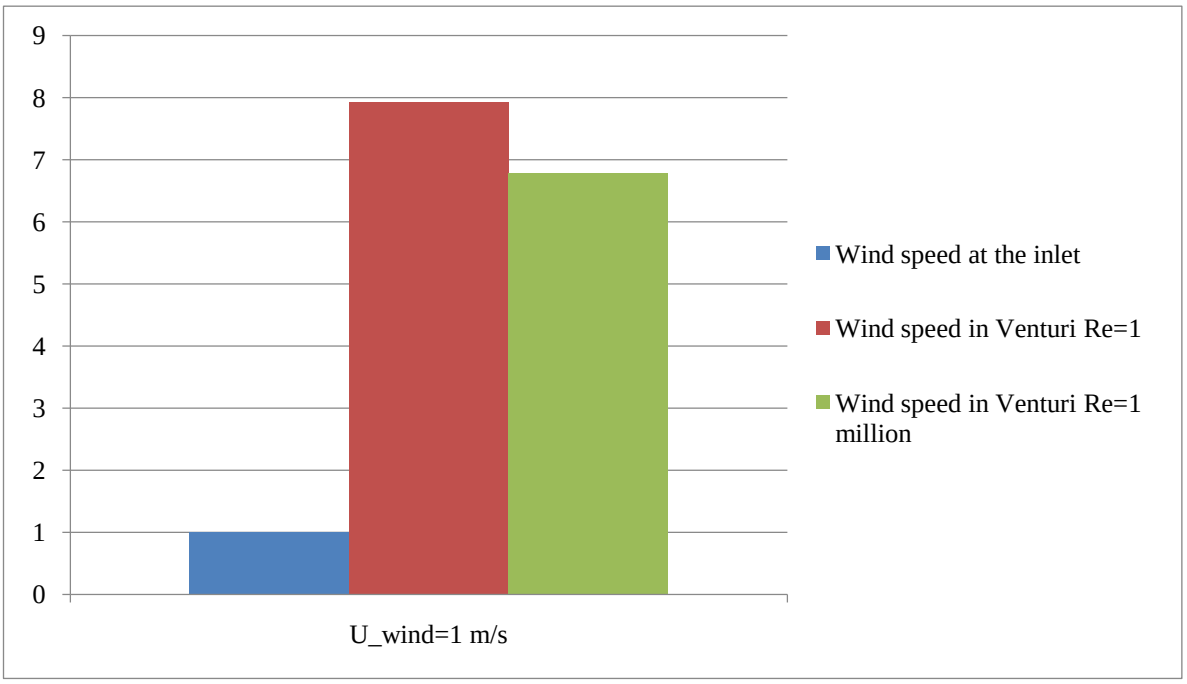

Figure 11.2 - Comparison of wind speed in Model 2at the inlet and outlets in dependence of Reynolds number

From the graph 11.1 we know that the highest wind speed for model 2 was reached for Reynolds number equals 1. The wind speed at the inlet was increased about almost 8 times. These result is much better than in case of model 1 but we need to take into account that model 2 is not omnidirectional. There should be applied the system of revolution control what seems to be uneconomical and impractical when we have to deal with the wind blowing from different directions and not primarily one.

12. CONSLUSIONS

As we can see at the Figure 10.7 the increase of wind speed in Venturi is significant. In case of model 1 it has increased 3 times, up to 3.7. The lowest speed of wind which is used by the turbine is 4 and the higher 25. This values strictly depends of diameter of the turbine. The INVELOX system let us to create the environment of higher wind speed and applied wind turbine with smaller diameter of blades. In addition to material saving (composites where recycling is not possible), the construction of INVELOX will be secured environment form the negative effects of turbines. The INVELOX housing allows to decrease a risk of collision with the birds, eliminate the flickering lights and mute the noise and vibration of turbine.

During the selection of kind of the turbine and additional support systems we need to take into account the demand of energy that we need to receive.

COMSOL Multiphysics is a really useful tool for both calculations of fluid mechanics and other fields of engineering. Program allows to create good quality model and study it with complex conditions. Taking into account the complexity of fluid mechanic necessary was to set up several simplifications which make easier the calculation.

BIBLIOGRAPHY

1] Stanisław Drobniak, Mechanika Płynów, Grudzień 2008.

2] K. Jeżowiecka-Kabsch, Henryk Szewczyk, Mechanika Płynów, Oficyna Wydawnicza Politechniki Wrocławskiej Wrocław, 1998.

3] R. Gryboś, Mechanika Płynów, Wydanie VII, Gliwice, 1991.

4] M. Griebel, T. Dornseifer, and T. Neunhoeffer. Numerical Simulation in Fluid Dynamics: A Practical Introduction. Society for Industrial and Applied Mathematics, Philadelphia, 1998..

5] Introduction to COMSOL Multiphysics, 1998-2015 COMSOL

6] Szymon Liszka, Sławomir Pasierb, Energetyka a zmiany klimatu, Insytut na rzecz Ekorozwoju, Warszawa 2008.

7] Anna Grzybek, Odnawialne źródła energii i działania adaptacyjne do zmian klimatu w rolnictwie i na wsi – przykłady doświadczeń w UE, Scholar, Warszawa 2009.

8] Frank M. White, Fuscous Fluid Flow, Mc-Graw Hill, 1991.

9] Roland W. Lewis, Perumal Nithiarasu, Kankanhally N. Seetharamu, Fundamentals of the Finite Element Method for Heat and Fluid Flow, Wiley, 2004.

10] https://wszechswiatnauki.wordpress.com/

11] http://sheerwind.com/technology

12] http://www.sciencedirect.com/science/article/pii/S0360544214002837

STRESZCZENIE

W pracy przedstawiony został przewidywany rozwój energetyki odnawialnej, w szczególności energii wiatrowej, na świecie. W następnej kolejności opisano nowoczesny system INXELOX, którego zadaniem jest przechwycenie siły wiatru, jej kumulacja i przyśpieszenie w kluczowym elemencie systemu jakim jest zwężenie Venturi. Dzięki temu rozwiązaniu istnieje możliwość zwiększenia siły wiatru ponad trzykrotnie.

W dalszej części pracy przestawione zostały równania Navier-Stokes'a zarówno w formie wymiarowej jak i bezwymiarowej.

W następnym rozdziale 5 przedstawiono model 2D Systemu INVELOX wykonany w programie Solidworks, po zastosowanym skalowaniu wymiarów do wymiaru charakterystycznego jakim jest średnica zwężenia Venturi D.

W dalszej części pracy omówiono sposób programowania symulacji w programie COMSOL Multiphysics. Opisane zostały kroki niezbędne do poprawnego wykonania symulacji. W pierwszej kolejności opisano parametryzacje wartości, np. prędkości wiejącego wiatru. Kolejno omówiono model i sposób definiowania parametrów materiału z którego został wykonany – w tym przypadku powietrza. Następnie pokazany został sposób nakładania warunków brzegowych na dane krawędzie modelu oraz warunków brzegowych warstwowych na wewnętrzną część zwężenia Venturi.

W następnym rozdziale umieszczono wyniki symulacji zależnej i niezależnej od czasu. Zamieszczono wykresy rozkładu pól prędkości i ciśnień z zastosowaniem różnych wartości liczby Reynoldsa dla obydwu przypadków. Dla symulacji zależnych od czasu przedstawiono wyniki wygenerowane w 0s, 5s i 10s symulacji.

W rozdziale 8 zaprezentowano drugi model 2 poddany symulacji. Podobnie jak w przypadku modelu 1 przedstawiono sposób programowania jego symulacji i rodzaj wygenerowanej siatki. Wykonano symulacje zależną od czasu i niezależną. W obydwu zawarto wykresy pól prędkości wiatru i rozkładu ciśnień.

Na koniec wykonano wykres porównujący maksymalne osiągnięte prędkości przepływu wiatru w zwężeniu dla obydwu modeli w porównaniu do prędkości wejściowej na wlocie.